Chapter 11

CONSTITUTIVE MODELING OF INTERFACIAL AREA TRANSPORT

The two-fluid model is widely used in the current two-phase flow analysis codes, such as nuclear reactor safety analysis codes RELAP5, TRAC, and CATHARE. In the conventional model, the interfacial area concentration is given by empirical correlations. The correlations are based on two-phase flow regimes and regime-transition criteria that do not dynamically represent the changes in interfacial structure. There exist the following shortcomings caused by this static approach.

1. The flow-regime transition criteria are algebraic relations for steady-state, fully-developed flow. They do not fully reflect the true dynamic nature of changes in the interfacial structure. Hence, the effects of the entrance and developing flow cannot be taken into account correctly, nor can the gradual transition between regimes.
2. The method based on the flow-regime transition criteria is a two-step method that requires flow configuration transition criteria and interfacial area correlations for each flow configuration. The compound errors from the transition criteria and interfacial area correlations can be very significant.
3. The transition criteria and flow-regime dependent interfacial correlations are valid in limited parameter ranges for certain specific operational conditions and geometries. Most of them are obtained from simple air-water experiments and phenomenological models. Often the scale effects of geometry and fluid properties are not correctly taken into account. When applied to high-to-low pressure steam-water transients, these models may cause significant discrepancies, artificial discontinuities and numerical instability.

In Chapter 10, a physics-based approach, namely the interfacial area transport equation, was introduced to dynamically obtain the interfacial area concentration. In bubbly flow regime, bubbles may be assumed close to spherical in shape and with similar size, and thus a one-group interfacial area transport equation is sufficient to describe the interfacial area transport phenomena. However, in more generalized gas-liquid two-phase flows such as cap bubbly, slug and churn-turbulent flows, there exist bubbles with different sizes and shapes such as spherical, distorted, cap, slug, or churn-turbulent bubble. These variations in bubble size and shape substantially affect the bubble transport phenomena due to the differences in drag force and bubble interaction mechanisms. In developing the transport equation applicable to a wide range of two-phase flow, the differences in the shape and size of bubbles and in the characteristic transport phenomena should be accounted for. In view of this, the bubbles are categorized into two groups: spherical/distorted bubbles as Group 1 and cap/slug/churn-turbulent bubbles as Group 2. In Chapter 10, a general approach to treat bubbles in two groups was presented and the two-group interfacial area transport equation was formulated. In implementing the two-group interfacial area transport equation to the two-fluid model, some modifications of the conventional two-fluid model are required. This is mainly because the introduction of the two groups of bubbles requires two gas velocity fields while the conventional two-fluid model only provides one gas velocity through the momentum equation.

This chapter presents the modified two-fluid model that is ready to be implemented in the approach of the two-group interfacial area transport equation. Two momentum equations can be written for the two groups of bubbles, although it is not yet very practical to solve two gas momentum equations. However, for fully three-dimensional flow this may be necessary, whereas for one-dimensional flow a simplified approach is proposed. In this case, the momentum equation for the averaged velocity of the gas-phase is retained by combining the two gas momentum equations. Additional terms related to the velocity difference between Group-1 and Group-2 bubbles should be specified. This velocity difference can be estimated based on the simplified momentum equations for both Group-1 and Group-2 bubbles by accounting for the pressure gradient and general drag force. Furthermore, in one-dimensional simplification, a modified drift-flux model may be applied to solve for the velocity difference. In addition to this, this chapter demonstrates the modeling of sink and source terms in one-group and two-group interfacial area transport equations.

1.1 Modified two-fluid model for the two-group interfacial area transport equation

1.1.1 Conventional two-fluid model

As discussed in Chapter 9, a three-dimensional two-fluid model has been obtained by using temporal or statistical averaging. The model is expressed in terms of two sets of conservation equations governing the balance of mass, momentum and energy in each phase. However, since the averaged fields of one phase are not independent of the other phase, the interaction terms appear in the field equations as source terms. For most practical applications, the two-fluid model can be simplified to the following forms (Ishii, 1977; Ishii and Mishima, 1984) from Chapter 9.

Continuity equation for the gas phase

$$\frac{\partial\left(\alpha_g\rho_g\right)}{\partial t}+\nabla\cdot\left(\alpha_g\rho_g\boldsymbol{v}_g\right)=\Gamma_g \tag{11-1}$$

Continuity equation for the liquid phase

$$\frac{\partial\left[\left(1-\alpha_g\right)\rho_f\right]}{\partial t}+\nabla\cdot\left[\left(1-\alpha_g\right)\rho_f\boldsymbol{v}_f\right]=\Gamma_f \tag{11-2}$$

Momentum equation for the gas phase

$$\begin{aligned}&\frac{\partial\left(\alpha_g\rho_g\boldsymbol{v}_g\right)}{\partial t}+\nabla\cdot\left(\alpha_g\rho_g\boldsymbol{v}_g\boldsymbol{v}_g\right)=-\alpha_g\nabla p_g\\&+\nabla\cdot\left[\alpha_g\left(\mathbb{T}_g^{\mu}+\mathbb{T}_g^{T}\right)\right]+\alpha_g\rho_g\boldsymbol{g}\\&+\Gamma_g\boldsymbol{v}_{gi}+\boldsymbol{M}_{ig}-\nabla\alpha_g\cdot\mathbb{T}_{gi}+\left(p_{gi}-p_g\right)\nabla\alpha_g\end{aligned} \tag{11-3}$$

Momentum equation for the liquid phase

$$\begin{aligned}&\frac{\partial\left[\left(1-\alpha_g\right)\rho_f\boldsymbol{v}_f\right]}{\partial t}+\nabla\cdot\left[\left(1-\alpha_g\right)\rho_f\boldsymbol{v}_f\boldsymbol{v}_f\right]=-\left(1-\alpha_g\right)\nabla p_f\\&+\nabla\cdot\left[\left(1-\alpha_g\right)\left(\mathbb{T}_f^{\mu}+\mathbb{T}_f^{T}\right)\right]+\left(1-\alpha_g\right)\rho_f\boldsymbol{g}\\&+\Gamma_f\boldsymbol{v}_{fi}+\boldsymbol{M}_{if}-\nabla\left(1-\alpha_g\right)\cdot\mathbb{T}_{fi}+\left(p_{fi}-p_f\right)\nabla\left(1-\alpha_g\right)\end{aligned} \tag{11-4}$$

Thermal energy equation for the gas phase

$$\frac{\partial\left(\alpha_g\rho_g h_g\right)}{\partial t}+\nabla\cdot\left(\alpha_g\rho_g h_g \boldsymbol{v}_g\right)=-\nabla\cdot\left[\alpha_g\left(\boldsymbol{q}_g^C+\boldsymbol{q}_g^T\right)\right]$$
$$+\alpha_g\frac{D_g p_g}{Dt}+\left(p_g-p_{gi}\right)\frac{D_g\alpha_g}{Dt}+\Gamma_g h_{gi}+a_i q_{gi}''+\phi_g \tag{11-5}$$

Thermal energy equation for the liquid phase

$$\frac{\partial\left[\left(1-\alpha_g\right)\rho_f h_f\right]}{\partial t}+\nabla\cdot\left[\left(1-\alpha_g\right)\rho_f \boldsymbol{v}_f h_f\right]$$
$$=-\nabla\cdot\left[\left(1-\alpha_g\right)\left(\boldsymbol{q}_f^C+\boldsymbol{q}_f^T\right)\right]+\left(1-\alpha_g\right)\frac{D_f p_f}{Dt} \tag{11-6}$$
$$+\left(p_f-p_{fi}\right)\frac{D_f\left(1-\alpha_g\right)}{Dt}+\Gamma_f h_{fi}+a_i q_{fi}''+\phi_f$$

Here, Γ_k, $\boldsymbol{M}_{ik}$, $\overline{\overline{\mathcal{T}}}_{ki}$, q_{ki}'' and ϕ_k are the mass generation, the generalized interfacial drag, the interfacial shear stress, the interfacial heat flux, and the dissipation, respectively. For simplicity, in the above equations the mathematical symbols of averaging are dropped, and $\overline{\overline{\mathcal{T}}}_k$, $\overline{\overline{\mathcal{T}}}_{ki}$ and $\overline{\overline{\boldsymbol{q}}}_k$ are represented by $\mathcal{T}_k^{\mu}$, $\mathcal{T}_{ki}$ and $\boldsymbol{q}_k^C$.

In Eqs.(11-1) to (11-6), the generation of mass per unit volume, the generalized drag force per unit volume, and the interfacial energy transfer per unit volume constitute the interfacial transfer terms. The jump conditions for the interfacial transfers are given as

$$\begin{cases}\Gamma_g+\Gamma_f=0\\ \boldsymbol{M}_{ig}+\boldsymbol{M}_{if}=0\\ \left(a_i q_{gi}''+\Gamma_g h_{gi}\right)+\left(a_i q_{fi}''+\Gamma_f h_{fi}\right)=0.\end{cases} \tag{11-7}$$

1.1.2 Two-group void fraction and interfacial area transport equations

The two-group void fraction transport equation is given by

$$\frac{\partial\left(\alpha_{gk}\rho_g\right)}{\partial t}+\nabla\cdot\left(\alpha_{gk}\rho_g\boldsymbol{v}_{gk}\right)=\Gamma_{gk}+(-1)^k\,\Delta\dot{m}_{12} \tag{11-8}$$

where k =1 and 2 for Groups 1 and 2, respectively. Γ_{gk} is the mass generation rate of Group-k bubbles due to phase change, and $\Delta\dot{m}_{12}$ represents the net inter-group mass transfer rate from Group-1 to Group-2 bubbles due to the bubble interactions and the hydrodynamic effect given by

$$\Delta\dot{m}_{12}=\rho_g\left[\sum_j\eta_{j,2}+\chi\left(D_{c1}^*\right)^3\left\{\frac{\partial\alpha_{g1}}{\partial t}+\nabla\cdot\left(\alpha_{g1}\boldsymbol{v}_{g1}\right)-\eta_{ph1}\right\}\right] \tag{11-9}$$

where $\eta_{j,2}$ and η_{phk} are the net inter-group void fraction transport from Group-1 to Group-2 bubbles and the source and sink term for the gas volume due to phase change, respectively. χ is the inter-group transfer coefficient and D_{c1}^* is the non-dimensional bubble diameter defined by

$$D_{c1}^*\equiv\frac{D_{crit}}{D_{Sm1}} \tag{11-10}$$

where D_{crit} is the volume-equivalent diameter of a bubble at the boundary between Groups 1 and 2.

The two-group interfacial area transport equation is given by

$$\begin{aligned}&\frac{\partial a_{i1}}{\partial t}+\nabla\cdot\left(a_{i1}\boldsymbol{v}_{gi1}\right)\\&=\left\{\frac{2}{3}-\chi\left(D_{c1}^*\right)^2\right\}\frac{a_{i1}}{\alpha_{g1}}\left[\frac{\partial\alpha_{g1}}{\partial t}+\nabla\cdot\left(\alpha_{g1}\boldsymbol{v}_{g1}\right)-\eta_{ph1}\right]\\&+\sum_j\phi_{j,1}+\phi_{ph1}\end{aligned} \tag{11-11}$$

$$\begin{aligned}&\frac{\partial a_{i2}}{\partial t}+\nabla\cdot\left(a_{i2}\boldsymbol{v}_{gi2}\right)=\frac{2}{3}\frac{a_{i2}}{\alpha_{g2}}\left[\frac{\partial\alpha_{g2}}{\partial t}+\nabla\cdot\left(\alpha_{g2}\boldsymbol{v}_{g2}\right)-\eta_{ph2}\right]\\&+\chi\left(D_{c1}^*\right)^2\frac{a_{i1}}{\alpha_{g1}}\left[\frac{\partial\alpha_{g1}}{\partial t}+\nabla\cdot\left(\alpha_{g1}\boldsymbol{v}_{g1}\right)-\eta_{ph1}\right]\\&+\sum_j\phi_{j,2}+\phi_{ph2}\end{aligned} \tag{11-12}$$

where $\phi_{j,k}$ and ϕ_{phk} are the source and sink terms for the interfacial area concentration due to bubble interactions for Group-*k* bubbles and phase change, respectively.

1.1.3 Modified two-fluid model

In what follows, the two-fluid model is modified for two-group interfacial area transport equation (Sun et al., 2003). The general form is given by the multi-field model for the gas phase. In general, the pressure and temperature for Group-1 and Group-2 bubbles can be assumed to be approximately the same. However, the velocities of two groups are not the same, therefore it is necessary to introduce two continuity and two momentum equations in principle. Based on the above assumption, the density of the gas phase is the same for Group-1 and Group-2 bubbles. This leads to the gas phase continuity equations as

Continuity equation for Group-1 bubbles

$$\frac{\partial\left(\alpha_{g1}\rho_g\right)}{\partial t}+\nabla\cdot\left(\alpha_{g1}\rho_g\boldsymbol{v}_{g1}\right)=\Gamma_{g1}-\Delta\dot{m}_{12} \tag{11-13}$$

Continuity equation for Group-2 bubbles

$$\frac{\partial\left(\alpha_{g2}\rho_g\right)}{\partial t}+\nabla\cdot\left(\alpha_{g2}\rho_g\boldsymbol{v}_{g2}\right)=\Gamma_{g2}+\Delta\dot{m}_{12}. \tag{11-14}$$

Here, $\Delta\dot{m}_{12}$ is the inter-group mass transfer due to hydrodynamic mechanisms. Furthermore, if the following identities are introduced,

$$\begin{cases}\alpha_{g1}+\alpha_{g2}=\alpha_g\\ \Gamma_{g1}+\Gamma_{g2}=\Gamma_g\\ \boldsymbol{v}_g=\dfrac{\left(\alpha_{g1}\boldsymbol{v}_{g1}+\alpha_{g2}\boldsymbol{v}_{g2}\right)}{\alpha_g}\end{cases} \tag{11-15}$$

then the summation of Eqs.(11-13) and (11-14) recovers the conventional continuity equation, i.e. Eq.(11-1). The continuity equation for the liquid phase remains the same as Eq.(11-2) with

$$\Gamma_f = -\Gamma_g = -\left(\Gamma_{g1} + \Gamma_{g2}\right). \tag{11-16}$$

The momentum equation is more complicated due to the introduction of the two groups of bubbles. Unlike the continuity equation for the gas phase, it is not desirable to have two momentum equations for Group-1 and Group-2 bubbles due to the complicated nature of the momentum equation at least for the one-dimensional formulation. If we assume Group-2 bubbles as the "third phases" in addition to the liquid phase and Group-1 bubbles and neglects the direct momentum interactions between the Group-1 and Group-2 bubbles, then two momentum equations may be written for both Group-1 and Group-2 bubbles as

$$\begin{aligned}
&\frac{\partial\left(\alpha_{g1}\rho_g \boldsymbol{v}_{g1}\right)}{\partial t} + \nabla\cdot\left(\alpha_{g1}\rho_g \boldsymbol{v}_{g1}\boldsymbol{v}_{g1}\right) = -\alpha_{g1}\nabla p_{g1} \\
&+\nabla\cdot\left[\alpha_1\left(\mathbb{T}_{g1}^{\mu} + \mathbb{T}_{g1}^{T}\right)\right] + \alpha_{g1}\rho_g \boldsymbol{g} + \left(\Gamma_{g1} - \Delta\dot{m}_{12}\right)\boldsymbol{v}_{gi1} \\
&-\nabla\alpha_1\cdot\mathbb{T}_{gi1} + \boldsymbol{M}_{ig1} + \left(p_{gi1} - p_{g1}\right)\nabla\alpha_{g1}
\end{aligned} \tag{11-17}$$

and

$$\begin{aligned}
&\frac{\partial\left(\alpha_{g2}\rho_g \boldsymbol{v}_{g2}\right)}{\partial t} + \nabla\cdot\left(\alpha_{g2}\rho_g \boldsymbol{v}_{g2}\boldsymbol{v}_{g2}\right) = -\alpha_2\nabla p_{g2} \\
&+\nabla\cdot\left[\alpha_2\left(\mathbb{T}_{g2}^{\mu} + \mathbb{T}_{g2}^{T}\right)\right] + \alpha_{g2}\rho_g \boldsymbol{g} + \left(\Gamma_{g2} + \Delta\dot{m}_{12}\right)\boldsymbol{v}_{gi2} \\
&-\nabla\alpha_2\cdot\mathbb{T}_{gi2} + \boldsymbol{M}_{ig2} + \left(p_{gi2} - p_{g2}\right)\nabla\alpha_{g2}.
\end{aligned} \tag{11-18}$$

Then, combining Eqs.(11-17) and (11-18) yields

$$\begin{aligned}
&\frac{\partial\left(\alpha_g\rho_g \boldsymbol{v}_g\right)}{\partial t} + \nabla\cdot\left(\alpha_g\rho_g \boldsymbol{v}_g\boldsymbol{v}_g\right) \\
&= -\nabla\cdot\left[\rho_g\frac{\alpha_{g1}\alpha_{g2}}{\alpha_g}\left(\boldsymbol{v}_{g1} - \boldsymbol{v}_{g2}\right)^2\right] - \left(\alpha_{g1}\nabla p_{g1} + \alpha_{g2}\nabla p_{g2}\right) \\
&+\nabla\cdot\left[\alpha_{g1}\left(\mathbb{T}_{g1}^{\mu} + \mathbb{T}_{g1}^{T}\right) + \alpha_{g2}\left(\mathbb{T}_{g2}^{\mu} + \mathbb{T}_{g2}^{T}\right)\right] + \alpha_g\rho_g \boldsymbol{g} \\
&+\left(p_{gi1} - p_{g1}\right)\nabla\alpha_{g1} + \left(p_{gi2} - p_{g2}\right)\nabla\alpha_{g2} \\
&+\left[\left(\Gamma_{g1} - \Delta\dot{m}_{12}\right)\boldsymbol{v}_{gi1} + \left(\Gamma_{g2} + \Delta\dot{m}_{12}\right)\boldsymbol{v}_{gi2}\right]
\end{aligned} \tag{11-19}$$

$$-\left(\nabla\alpha_1\cdot\mathbb{T}_{gi1}+\nabla\alpha_2\cdot\mathbb{T}_{gi2}\right)+\left(\boldsymbol{M}_{ig1}+\boldsymbol{M}_{ig2}\right)$$

with the definitions in Eq.(11-15). It is interesting to note that the first term on the right-hand side of Eq.(11-19) is an additional diffusion term due to the difference between the bubble velocities in different bubble groups.

However, Eq.(11-19) is too complicated to be applied in general applications. As mentioned earlier, for most of the practical applications, the pressure for the two groups of bubbles can be approximated as the same such that

$$p_{g1}\approx p_{g2}=p_g;\quad p_{gi1}\approx p_{gi2}=p_{gi}. \tag{11-20}$$

Furthermore, the interfacial shear for both groups of bubbles may be assumed to be very similar such that,

$$\mathbb{T}_{gi1}\approx\mathbb{T}_{gi2}=\mathbb{T}_{gi}. \tag{11-21}$$

We also have the following definition to further simplify Eq.(11-19)

$$\begin{cases}\mathbb{T}_g\equiv\dfrac{\alpha_{g1}\mathbb{T}_{g1}+\alpha_{g2}\mathbb{T}_{g2}}{\alpha_g}=\mathbb{T}_g^{\mu}+\mathbb{T}_g^{T}\\ \mathbb{T}_g^{\mu}\equiv\dfrac{\alpha_{g1}\mathbb{T}_{g1}^{\mu}+\alpha_{g2}\mathbb{T}_{g2}^{\mu}}{\alpha_g}\\ \mathbb{T}_g^{T}\equiv\dfrac{\alpha_{g1}\mathbb{T}_{g1}^{T}+\alpha_{g2}\mathbb{T}_{g2}^{T}}{\alpha_g}\\ \mathbb{T}_{g1}\equiv\mathbb{T}_{g1}^{\mu}+\mathbb{T}_{g1}^{T}\\ \mathbb{T}_{g2}\equiv\mathbb{T}_{g2}^{\mu}+\mathbb{T}_{g2}^{T}.\end{cases} \tag{11-22}$$

Therefore, Eq.(11-19) can be simplified as

$$\begin{aligned}&\frac{\partial\left(\alpha_g\rho_g\boldsymbol{v}_g\right)}{\partial t}+\nabla\cdot\left(\alpha_g\rho_g\boldsymbol{v}_g\boldsymbol{v}_g\right)=-\nabla\cdot\left[\rho_g\frac{\alpha_{g1}\alpha_{g2}}{\alpha_g}\left(\boldsymbol{v}_{g1}-\boldsymbol{v}_{g2}\right)^2\right]\\&-\alpha_g\nabla p_g+\nabla\cdot\left[\alpha_g\left(\mathbb{T}_g^{\mu}+\mathbb{T}_g^{T}\right)\right]+\alpha_g\rho_g\boldsymbol{g}\end{aligned} \tag{11-23}$$

$$+\left[\left(\Gamma_{g1}-\Delta\dot{m}_{12}\right)\boldsymbol{v}_{gi1}+\left(\Gamma_{g2}+\Delta\dot{m}_{12}\right)\boldsymbol{v}_{gi2}\right]-\nabla\alpha_g\cdot\mathbb{T}_{gi}$$
$$+\left(\boldsymbol{M}_{ig1}+\boldsymbol{M}_{ig2}\right)+\left(p_{gi}-p_g\right)\nabla\alpha_g.$$

It may be reasonable to assume that the averaged stresses in the bulk fluid and at the interface are approximately the same. Thus,

$$\mathbb{T}_{gi}\approx\left(\mathbb{T}_g^{\mu}+\mathbb{T}_g^{T}\right). \tag{11-24}$$

Then, Eq.(11-23) is further simplified as

$$\frac{\partial\left(\alpha_g\rho_g\boldsymbol{v}_g\right)}{\partial t}+\nabla\cdot\left(\alpha_g\rho_g\boldsymbol{v}_g\boldsymbol{v}_g\right)=-\nabla\cdot\left[\rho_g\frac{\alpha_{g1}\alpha_{g2}}{\alpha_g}\left(\boldsymbol{v}_{g1}-\boldsymbol{v}_{g2}\right)^2\right]$$
$$-\alpha_g\nabla p_g+\alpha_g\nabla\cdot\left(\mathbb{T}_g^{\mu}+\mathbb{T}_g^{T}\right)+\alpha_g\rho_g\boldsymbol{g} \tag{11-25}$$
$$+\left[\Gamma_{g1}\boldsymbol{v}_{g1}+\Gamma_{g2}\boldsymbol{v}_{g2}+\Delta\dot{m}_{12}\left(\boldsymbol{v}_{g2}-\boldsymbol{v}_{g1}\right)\right]+\left(\boldsymbol{M}_{ig1}+\boldsymbol{M}_{ig2}\right)$$
$$+\left(p_{gi}-p_g\right)\nabla\alpha_g.$$

The generalized interfacial drag terms, $\boldsymbol{M}_{ig1}$ and $\boldsymbol{M}_{ig2}$, should be individually modeled for Group-1 and Group-2 bubbles.

Furthermore, the momentum equation for the liquid phase has the same form as Eq.(11-3). Thus,

$$\frac{\partial\left[\left(1-\alpha_g\right)\rho_f\boldsymbol{v}_f\right]}{\partial t}+\nabla\cdot\left[\left(1-\alpha_g\right)\rho_f\boldsymbol{v}_f\boldsymbol{v}_f\right]=-\left(1-\alpha_g\right)\nabla p_f$$
$$+\nabla\cdot\left[\left(1-\alpha_g\right)\left(\mathbb{T}_f^{\mu}+\mathbb{T}_f^{T}\right)\right]+\left(1-\alpha_g\right)\rho_f\boldsymbol{g} \tag{11-26}$$
$$+\Gamma_f\boldsymbol{v}_{fi}+\boldsymbol{M}_{if}-\nabla\left(1-\alpha_g\right)\cdot\mathbb{T}_{fi}+\left(p_{fi}-p_f\right)\nabla\left(1-\alpha_g\right)$$

with

$$\boldsymbol{M}_{if}=-\boldsymbol{M}_{ig}=-\left(\boldsymbol{M}_{ig1}+\boldsymbol{M}_{ig2}\right). \tag{11-27}$$

It may be reasonable to assume that the averaged stresses in the liquid phase and at the interface are approximately the same. Thus,

$$\mathbb{T}_{fi} \approx \left(\mathbb{T}_f^{\mu} + \mathbb{T}_f^{T}\right). \tag{11-28}$$

Then, Eq.(11-26) is further simplified as

$$\begin{aligned}
&\frac{\partial\left[\left(1-\alpha_g\right)\rho_f \boldsymbol{v}_f\right]}{\partial t} + \nabla\cdot\left[\left(1-\alpha_g\right)\rho_f \boldsymbol{v}_f \boldsymbol{v}_f\right] = -\left(1-\alpha_g\right)\nabla p_f \\
&+\left(1-\alpha_g\right)\nabla\cdot\left(\mathbb{T}_f^{\mu} + \mathbb{T}_f^{T}\right) + \left(1-\alpha_g\right)\rho_f \boldsymbol{g} \\
&+\Gamma_f \boldsymbol{v}_{fi} + \boldsymbol{M}_{if} + \left(p_{fi} - p_f\right)\nabla\left(1-\alpha_g\right).
\end{aligned} \tag{11-29}$$

In the above derivation, it is assumed that the pressures and the temperatures for the two groups of bubbles are essentially the same. Then, similar to the momentum equation, the thermal energy equation for the gas phase can be expressed as

$$\begin{aligned}
&\frac{\partial\left(\alpha_g\rho_g h_g\right)}{\partial t} + \nabla\cdot\left(\alpha_g\rho_g h_g \boldsymbol{v}_g\right) = -\nabla\cdot\left[\alpha_g\left(\boldsymbol{q}_g^{C} + \boldsymbol{q}_g^{T}\right)\right] \\
&+\alpha_g\frac{D_g p_g}{Dt} + \Gamma_g h_{gi} + a_i q_{gi}'' + \phi_g
\end{aligned} \tag{11-30}$$

where the following definitions have been applied

$$\begin{cases}
\boldsymbol{q}_g^{C} = \dfrac{\alpha_{g1}\boldsymbol{q}_{g1}^{C} + \alpha_{g2}\boldsymbol{q}_{g2}^{C}}{\alpha_g} \\
\boldsymbol{q}_g^{T} = \dfrac{\alpha_{g1}\boldsymbol{q}_{g1}^{T} + \alpha_{g2}\boldsymbol{q}_{g2}^{T}}{\alpha_g} \\
q_{gi}'' = \dfrac{a_{i1}q_{gi1}'' + a_{i2}q_{gi2}''}{a_i} \\
a_i = a_{i1} + a_{i2}.
\end{cases} \tag{11-31}$$

The operator D_g/Dt is defined as

$$\frac{D_g}{Dt} \equiv \frac{\partial}{\partial t} + \frac{\alpha_{g1}\boldsymbol{v}_{g1} + \alpha_{g2}\boldsymbol{v}_{g2}}{\alpha_{g1} + \alpha_{g2}}\cdot\nabla = \frac{\partial}{\partial t} + \boldsymbol{v}_g\cdot\nabla. \tag{11-32}$$

Similarly, the thermal energy equation for the liquid phase is written as

$$\begin{aligned}&\frac{\partial\left[\left(1-\alpha_g\right)\rho_f h_f\right]}{\partial t}+\nabla\cdot\left[\left(1-\alpha_g\right)\rho_f \boldsymbol{v}_f h_f\right]\\&=-\nabla\cdot\left[\left(1-\alpha_g\right)\left(\boldsymbol{q}_f^C+\boldsymbol{q}_f^T\right)\right]+\left(1-\alpha_g\right)\frac{D_f p_f}{Dt}+\Gamma_f h_{fi}\\&+a_i q_{fi}''+\phi_f\end{aligned} \tag{11-33}$$

with the interfacial heat transfer at the liquid-phase side as

$$q_{fi}''=\frac{a_{i1}q_{fi1}''+a_{i2}q_{fi2}''}{a_i}. \tag{11-34}$$

Note that the following interfacial energetic condition should be satisfied

$$\left(a_i q_{gi}''+\Gamma_g h_{gi}\right)+\left(a_i q_{fi}''+\Gamma_f h_{fi}\right)=0. \tag{11-35}$$

In the above derivation, very complicated interfacial transfer terms are introduced. To solve the modified two-fluid model with the two-group interfacial area transport equation, various constitutive relations, interfacial transfer terms, and boundary conditions should be specified for the additional variables. These variables can be summarized as

$$\begin{aligned}&\Gamma_{g1},\Gamma_{g2},\Gamma_f,\Delta\dot{m}_{12},\\&\mathbb{T}_g^{\mu},\mathbb{T}_g^{T},\mathbb{T}_f^{\mu},\mathbb{T}_f^{T},\boldsymbol{M}_{ig1},\boldsymbol{M}_{ig2},\boldsymbol{M}_{if},\mathbb{T}_{gi},\mathbb{T}_{fi},\boldsymbol{v}_{gi1},\boldsymbol{v}_{gi2},\boldsymbol{v}_{fi},\boldsymbol{g}\text{ and}\\&\boldsymbol{q}_g^C,\boldsymbol{q}_f^C,\boldsymbol{q}_g^T,\boldsymbol{q}_f^T,q_{gi}'',q_{fi}'',h_{gi},h_{fi}.\end{aligned}$$

1.1.4 Modeling of two gas velocity fields

For strongly one-dimensional flow, the introduction of two gas momentum equations may bring in unnecessary complications. In this case, the gas mixture momentum equation and an additional constitutive relation specifying the relative velocity between Group-1 and Group-2 gas velocities is sufficient. It is important to ensure that doing so will not over-specify the unknowns since the number of unknowns should equal the number of available equations.

The difference of the bubble velocities may be related to the local slip as

$$\boldsymbol{v}_{g1} - \boldsymbol{v}_{g2} = \left(\boldsymbol{v}_{g1} - \boldsymbol{v}_f\right) - \left(\boldsymbol{v}_{g2} - \boldsymbol{v}_f\right) = \boldsymbol{v}_{r1} - \boldsymbol{v}_{r2}\,. \tag{11-36}$$

To obtain the local relative velocity between the gas phase and liquid phase, a similar approach to Ishii (1977) may be taken along the drift-flux model formulation.

The momentum equation for Group-1 bubbles, i.e. Eq.(11-17) can be written in the following form by substituting the continuity equation and considering the assumptions of Eqs.(11-20) and (11-21) and $p_g = p_{gi}$.

$$\begin{aligned}&\alpha_{g1}\rho_g\left(\frac{\partial \boldsymbol{v}_{g1}}{\partial t} + \boldsymbol{v}_{g1}\cdot\nabla\boldsymbol{v}_{g1}\right) = -\alpha_{g1}\nabla p_{g1} + \alpha_{g1}\nabla\cdot\mathbb{T}_{g1} \\ &+\alpha_{g1}\rho_g\boldsymbol{g} + \left(\Gamma_{g1} - \Delta\dot{m}_{12}\right)\left(\boldsymbol{v}_{gi1} - \boldsymbol{v}_{g1}\right) + \boldsymbol{M}_{ig1}\end{aligned} \tag{11-37}$$

Similarly, we obtain the momentum equations for both Group-2 bubbles and the liquid phase as

$$\begin{aligned}&\alpha_{g2}\rho_g\left(\frac{\partial \boldsymbol{v}_{g2}}{\partial t} + \boldsymbol{v}_{g2}\cdot\nabla\boldsymbol{v}_{g2}\right) = -\alpha_{g2}\nabla p_{g2} + \alpha_{g2}\nabla\cdot\mathbb{T}_{g2} \\ &+\alpha_{g2}\rho_g\boldsymbol{g} + \left(\Gamma_{g2} + \Delta\dot{m}_{12}\right)\left(\boldsymbol{v}_{gi2} - \boldsymbol{v}_{g2}\right) + \boldsymbol{M}_{ig2}\end{aligned} \tag{11-38}$$

and

$$\begin{aligned}&\left(1-\alpha_g\right)\rho_f\left(\frac{\partial \boldsymbol{v}_f}{\partial t} + \boldsymbol{v}_f\cdot\nabla\boldsymbol{v}_f\right) = -\left(1-\alpha_g\right)\nabla p_f \\ &+\left(1-\alpha_g\right)\nabla\cdot\mathbb{T}_f + \left(1-\alpha_g\right)\rho_f\boldsymbol{g} + \Gamma_f\left(\boldsymbol{v}_{fi} - \boldsymbol{v}_f\right) + \boldsymbol{M}_{if}.\end{aligned} \tag{11-39}$$

To obtain the local relative velocity correlation, we consider a special condition such as steady-state condition without phase change and with negligible-transverse pressure gradient. Without phase change effect, the interfacial velocity and the phase velocity for each phase can be considered equal, i.e.

$$\boldsymbol{v}_{gi1} \approx \boldsymbol{v}_{g1};\quad \boldsymbol{v}_{gi2} \approx \boldsymbol{v}_{g2};\quad \boldsymbol{v}_{fi} \approx \boldsymbol{v}_f. \tag{11-40}$$

And the pressure for each phase may be approximated as

$$p_g \approx p_f \approx p_m. \tag{11-41}$$

Under these approximations, for a nearly one-dimensional flow, the above momentum equations can be expressed as

$$\boldsymbol{M}_{ig1} \approx \alpha_{g1}\nabla p_m - \alpha_{g1}\nabla\cdot\boldsymbol{\mathcal{T}}_{g1} - \alpha_{g1}\rho_g\boldsymbol{g} \tag{11-42}$$

$$\boldsymbol{M}_{ig2} \approx \alpha_{g2}\nabla p_m - \alpha_{g2}\nabla\cdot\boldsymbol{\mathcal{T}}_{g2} - \alpha_{g2}\rho_g\boldsymbol{g} \tag{11-43}$$

and

$$\boldsymbol{M}_{if} \approx \left(1-\alpha_g\right)\nabla p_m - \left(1-\alpha_g\right)\nabla\cdot\boldsymbol{\mathcal{T}}_f - \left(1-\alpha_g\right)\rho_f\boldsymbol{g}. \tag{11-44}$$

From the interfacial force balance, i.e. Eq.(11-27), the summation of the above three equations yields

$$\nabla p_m - \boldsymbol{M}_{\tau m} - \rho_m\boldsymbol{g} \approx 0 \tag{11-45}$$

in which $\boldsymbol{M}_{\tau m}$ is the force associated with the mixture transverse stress gradient and given by

$$\begin{aligned}\boldsymbol{M}_{\tau m} &\equiv \left(\alpha_{g1}\nabla\cdot\boldsymbol{\mathcal{T}}_{g1} + \alpha_{g2}\nabla\cdot\boldsymbol{\mathcal{T}}_{g2}\right) + \left(1-\alpha_g\right)\nabla\cdot\boldsymbol{\mathcal{T}}_f \\ &= \alpha_{g1}\boldsymbol{M}_{\tau g1} + \alpha_{g2}\boldsymbol{M}_{\tau g2} + \left(1-\alpha_g\right)\boldsymbol{M}_{\tau f}\end{aligned} \tag{11-46}$$

with

$$\boldsymbol{M}_{\tau g1} = \nabla\cdot\boldsymbol{\mathcal{T}}_{g1}; \quad \boldsymbol{M}_{\tau g2} = \nabla\cdot\boldsymbol{\mathcal{T}}_{g2}; \quad \boldsymbol{M}_{\tau f} = \nabla\cdot\boldsymbol{\mathcal{T}}_f \tag{11-47}$$

while ρ_m is defined as

$$\rho_m \equiv \left(\alpha_{g1} + \alpha_{g2}\right)\rho_g + \left(1-\alpha_g\right)\rho_f = \alpha_g\rho_g + \left(1-\alpha_g\right)\rho_f. \tag{11-48}$$

Equation (11-45) also assumes that Eq.(11-28) is valid for most applications.

Furthermore, from Eq.(11-45), the gravitational force field may be replaced with the pressure field, which is an unknown in the momentum equation, as

$$\boldsymbol{g} \approx \frac{1}{\rho_m}(\nabla p_m - \boldsymbol{M}_{\tau m}). \tag{11-49}$$

This allows the approach to be applied in microgravity conditions. In steady state, the generalized interfacial drag force is approximated by neglecting the virtual mass force, the Basset force and non-drag force such as lift force as

$$\boldsymbol{M}_{ig1} \approx -\frac{3\alpha_{g1}}{8r_{d1}} C_{D1}\rho_f \boldsymbol{v}_{r1}|\boldsymbol{v}_{r1}| \tag{11-50}$$

where r_{d1} and C_{D1} are the drag radius and the drag coefficient of Group-1 bubble, and the relative velocity for Group-1 bubbles is defined as

$$\boldsymbol{v}_{r1} = \boldsymbol{v}_{g1} - \boldsymbol{v}_f. \tag{11-51}$$

Thus, in steady state, by using Eqs.(11-49) and (11-50), we can rewrite Eq.(11-42) as

$$\begin{aligned} &-\frac{3\alpha_{g1}}{8r_{d1}} C_{D1}\rho_f \boldsymbol{v}_{r1}|\boldsymbol{v}_{r1}| \\ &\approx \alpha_{g1}\left(1-\frac{\rho_g}{\rho_m}\right)\nabla p_m + \alpha_{g1}\left(\frac{\rho_g}{\rho_m}\boldsymbol{M}_{\tau m} - \boldsymbol{M}_{\tau g1}\right) \end{aligned} \tag{11-52}$$

or in the following form

$$\boldsymbol{v}_{r1}|\boldsymbol{v}_{r1}| \approx -\frac{8r_{d1}}{3C_{D1}\rho_f}\left[\left(1-\frac{\rho_g}{\rho_m}\right)\nabla p_m + \left(\frac{\rho_g}{\rho_m}\boldsymbol{M}_{\tau m} - \boldsymbol{M}_{\tau g1}\right)\right]. \tag{11-53}$$

Similarly, for Group-2 bubbles, we have the following formulation

$$\boldsymbol{v}_{r2}|\boldsymbol{v}_{r2}| \approx -\frac{8r_{d2}}{3C_{D2}\rho_f}\left[\left(1-\frac{\rho_g}{\rho_m}\right)\nabla p_m + \left(\frac{\rho_g}{\rho_m}\boldsymbol{M}_{\tau m} - \boldsymbol{M}_{\tau g2}\right)\right] \tag{11-54}$$

where r_{d2} and C_{D2} are the drag radius and the drag coefficient of Group-2 bubbles, respectively, and the relative velocity for Group-2 bubbles is defined as

$$\boldsymbol{v}_{r2} = \boldsymbol{v}_{g2} - \boldsymbol{v}_f. \tag{11-55}$$

From Eqs.(11-53) and (11-54), together with Eq.(11-36), we can solve the local slip between the two groups of bubbles, i.e. $\boldsymbol{v}_{g1} - \boldsymbol{v}_{g2}$.

In the case of one-dimensional flows, the one-dimensional drift-flux model to be discussed in Chapter 14 can be utilized to specify the velocity difference. The one-dimensional drift-flux model is modified for two-group interfacial area transport equation as

$$\left\langle\left\langle v_{gk}\right\rangle\right\rangle = C_{0k}\left\langle j\right\rangle + \left\langle\left\langle V_{gjk}\right\rangle\right\rangle \tag{11-56}$$

where $\left\langle\left\langle v_{gk}\right\rangle\right\rangle$, C_{0k} and $\left\langle\left\langle V_{gjk}\right\rangle\right\rangle$ are the void fraction weighted mean gas velocity, the distribution parameter, and the void fraction weighted mean drift velocity of Group-k bubbles, respectively. Then, the velocity difference is given by

$$\begin{aligned}\left\langle\left\langle v_{g1}\right\rangle\right\rangle - \left\langle\left\langle v_{g2}\right\rangle\right\rangle &= \left(\left\langle\left\langle v_{g1}\right\rangle\right\rangle - \left\langle j\right\rangle\right) - \left(\left\langle\left\langle v_{g2}\right\rangle\right\rangle - \left\langle j\right\rangle\right) \\ &= \left[(C_{01}-1)\left\langle j\right\rangle + \left\langle\left\langle V_{gj1}\right\rangle\right\rangle\right] - \left[(C_{02}-1)\left\langle j\right\rangle + \left\langle\left\langle V_{gj2}\right\rangle\right\rangle\right].\end{aligned} \tag{11-57}$$

The distribution parameters for both groups of bubbles should be obtained from experimental data for certain flow geometry. Furthermore, if we assume that the distribution parameters for both groups of bubbles are essentially similar for certain flows, then the following simplified form can be approximately obtained as

$$\left\langle\left\langle v_{g1}\right\rangle\right\rangle - \left\langle\left\langle v_{g2}\right\rangle\right\rangle \approx \left\langle\left\langle V_{gj1}\right\rangle\right\rangle - \left\langle\left\langle V_{gj2}\right\rangle\right\rangle. \tag{11-58}$$

1.2 Modeling of source and sink terms in one-group interfacial area transport equation

To model the integral source and sink terms in the interfacial area transport equation caused by particle coalescence and breakup, a general approach treats the bubbles in two groups: the spherical/distorted bubble group and the cap/slug bubble group, resulting in two interfacial area transport equations that involve the inner- and inter-group interactions as shown in Fig.11-1. As shown in Fig.11-2, the mechanisms of these interactions can be summarized in five categories: the coalescence due to random collisions driven by liquid turbulence; the coalescence due to wake

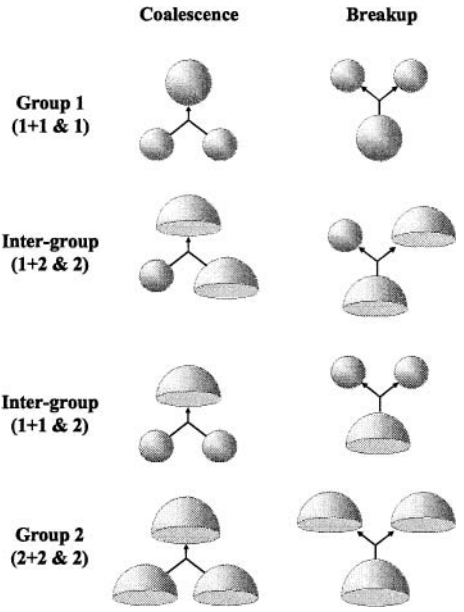

Figure 11-1. Classification of possible interactions of two-group bubbles (Hibiki and Ishii, 2000b)

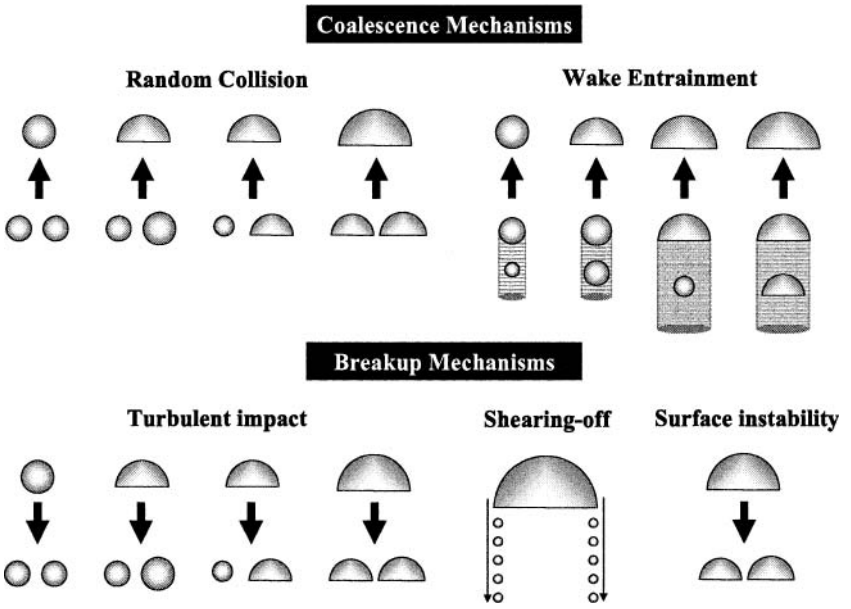

Figure 11-2. Schematic illustrations of two-group bubble interaction (Ishii et al., 2002)

entrainment; the breakup due to the impact of turbulent eddies; the shearing-off of small bubbles from cap/slug bubbles; and the breakup of large cap bubbles due to flow instability on the bubble surface (Kocamustafaogullari and Ishii, 1995; Wu et al., 1998). Some other mechanisms such as laminar-shearing induced coalescence (Friedlander, 1977) and the breakup due to velocity gradient (Taylor, 1934) are excluded because they are indirectly caused by the distributions of the flow parameters and void fraction, and the direct mechanisms still follow the above five categories.

In practice, when the void fraction of a two-phase bubbly flow is small, no cap or slug bubbles exist. The two-group interfacial area transport equation is then reduced to one group without the involvement of the interactions between the two groups as

$$\frac{\partial a_i}{\partial t} + \nabla \cdot \left(a_i \boldsymbol{v}_i\right) = \frac{2}{3}\left(\frac{a_i}{\alpha_g}\right)\left[\frac{\partial \alpha_g}{\partial t} + \nabla \cdot \left(\alpha_g \boldsymbol{v}_g\right) - \eta_{ph}\right] + \sum_j \phi_j + \phi_{ph}. \tag{11-59}$$

In this section, some models of source and sink terms in one-group interfacial area transport equation are explained briefly.

1.2.1 Source and sink terms modeled by Wu et al. (1998)

Wu et al. (1998) considered three mechanisms of the interfacial area transport in an adiabatic bubbly flow, namely coalescence due to random collisions driven by liquid turbulence, coalescence due to wake entrainment, and breakup due to the impact of turbulent eddies. Then, Eq.(11-59) is further simplified as

$$\frac{\partial a_i}{\partial t} + \nabla \cdot \left(a_i \boldsymbol{v}_i\right) = \frac{2}{3}\left(\frac{a_i}{\alpha_g}\right)\left[\frac{\partial \alpha_g}{\partial t} + \nabla \cdot \left(\alpha_g \boldsymbol{v}_g\right)\right] + \left(\phi_{RC} + \phi_{WE} + \phi_{TI}\right). \tag{11-60}$$

A. Bubble coalescence due to random collision

To model the bubble coalescence rate driven by turbulence in the continuous medium, the bubble random collision rate is of primary importance. These collisions are postulated to occur only between the neighboring bubbles because long-range interactions are driven by large

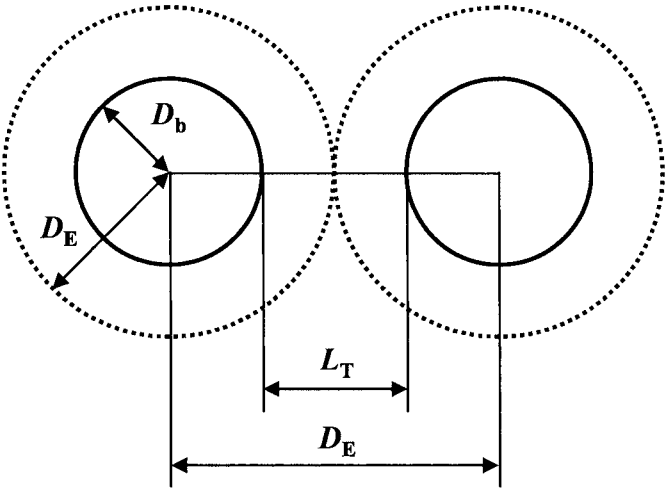

Figure 11-3. Geometric definitions of two approaching bubbles (Wu et al., 1998)

eddies that transport groups of bubbles without leading to significant relative motion (Prince and Blanch, 1990; Coulaloglou and Tavlarides, 1976). Between two neighboring spherical bubbles of the same size as shown in Fig.11-3, the time interval for one collision, Δt_C, is defined as

$$\Delta t_C = \frac{L_T}{u_t}. \tag{11-61}$$

Here, u_t is the root-mean-square approaching velocity of the two bubbles, and L_T represents the mean traveling distance between the two bubbles for one collision. This is approximated by

$$L_T \approx D_E - \delta D_b \propto \left(\frac{D_b}{\alpha_g^{1/3}} - \delta' D_b \right) = \frac{D_b}{\alpha_g^{1/3}} \left(1 - \delta' \alpha_g^{1/3} \right) \tag{11-62}$$

in which D_E is the effective diameter of the mixture volume that contains one bubble, and D_b is the bubble diameter. Since the bubble-traveling length for one collision varies from D_E to $\left(D_E - D_b\right)$, a factor δ is introduced in Eq.(11-62) to feature the averaged effect (whereas δ' is a collective parameter in considering the sign of proportionality between D_E and $D_b / \alpha_g^{1/3}$). For small void fraction, δ' plays a minor role due to the fact that D_E is much larger than D_b. However, it is important if the traveling length is comparable to the mean bubble size. When void fraction

approaches the dense packing limit $\left(\alpha_g \cong \alpha_{g,max}\right)$, the mean traveling length should be zero, which leads to δ' equal to $\alpha_{g,max}^{-1/3}$. Using this asymptotic value as the approximation of δ', the mean traveling length is reduced to

$$L_T \propto \frac{D_b}{\alpha_g^{1/3}}\left\{1-\left(\frac{\alpha_g}{\alpha_{g,max}}\right)^{1/3}\right\}. \tag{11-63}$$

Accordingly, the collision frequency for two bubbles moving toward each other, f_{RC}, is given by

$$f_{RC} = \frac{1}{\Delta t_C} \propto \frac{u_t}{D_b}\alpha_g^{1/3}\left(\frac{\alpha_{g,max}^{1/3}}{\alpha_{g,max}^{1/3}-\alpha_g^{1/3}}\right). \tag{11-64}$$

Since the bubbles do not always move toward each other, however, a probability, P_C, for a bubble to move toward a neighboring bubble is considered here to modify the collision rate. By assuming a hexagonal close-packed structure, this probability is given by

$$P_C \sim \frac{D_b^2}{D_E^2} = \alpha_g^{2/3},\ \alpha_g < \alpha_{g,crit} \text{ and } P_C = 1,\ \alpha_g > \alpha_{g,crit}. \tag{11-65}$$

where $\alpha_{g,crit}$ is the critical void fraction when the center bubble cannot pass through the free space among the neighboring bubbles. In reality, the neighboring bubbles are in constant motion and the critical void fraction can be very close to the dense packing limit. This leads to

$$P_C \propto \left(\frac{\alpha_g}{\alpha_{g,max}}\right)^{2/3}. \tag{11-66}$$

Subsequently, the collision frequency for a mixture with bubble number density, n_b, is given by

$$f_{RC} \approx \frac{1}{\Delta t_C}P_c \propto u_t\frac{\alpha_g}{D_b}\left\{\frac{1}{\alpha_{g,max}^{1/3}\left(\alpha_{g,max}^{1/3}-\alpha_g^{1/3}\right)}\right\} \tag{11-67}$$

$$\propto n_b u_t D_b^2 \left\{ \frac{1}{\alpha_{g,max}^{1/3}\left(\alpha_{g,max}^{1/3} - \alpha_g^{1/3}\right)} \right\}.$$

The functional dependence of the above collision rate agrees with the model of Coulaloglou and Tavlarides (1976) proposed for a liquid-liquid droplet flow system, analogous to the particle collision model in an ideal gas. The difference is that the present model contains an extra term in the bracket, which covers the situation when the mean-free path of a bubble is comparable to the mean bubble size. Nevertheless, the model in the present form is still incomplete, since no matter how far away the neighboring bubble is located, the collision would occur as long as there is a finite approaching velocity. In actuality, when the mean distance is very large, no collision should be counted because the range of the relative motion for collisions between the neighboring bubbles is limited by the eddy size comparable to the bubble size. To consider this effect, the following modification factor is suggested for Eq.(11-67)

$$\left\{1 - \exp\left(-C_T \frac{L_t}{L_T}\right)\right\}. \tag{11-68}$$

where C_T and L_t are, respectively, an adjustable parameter depending on the properties of the fluid and the average size of the eddies that drive the neighboring bubbles together. These eddies are assumed to be on the same order of the mean bubble size because smaller eddies do not provide considerable bulk motion to a bubble. Larger eddies, however, transport groups of bubbles without inducing significant relative motion among the bubbles. Thereafter, the final form of the bubble collision frequency is given by

$$\begin{aligned} f_{RC} \sim & \left(u_t n_b D_b^2\right)\left\{ \frac{1}{\alpha_{g,max}^{1/3}\left(\alpha_{g,max}^{1/3} - \alpha_g^{1/3}\right)} \right\} \\ & \times \left\{1 - \exp\left(-C_T \frac{\alpha_{max}^{1/3}\alpha^{1/3}}{\alpha_{max}^{1/3} - \alpha^{1/3}}\right)\right\}. \end{aligned} \tag{11-69}$$

For each collision, coalescence may not occur and thus a collision efficiency was suggested by many investigators (Oolman and Blanch,

1986b; Kirkpatrick and Lockett, 1974). The most popular model for the collision efficiency is the film thinning model (Kirkpatrick and Lockett, 1974). In this model, when the bubbles approach faster, they tend to bounce back without coalescence due to the limitation of the film-drainage rate governed by the surface tension. Mathematically, the coalescence rate decreases exponentially with respect to the turbulent fluctuating velocity, which is much stronger than the linear dependence of the collision rate, resulting in an overall decreasing trend of the coalescence rate as the turbulent fluctuation increases. Hence, a constant coalescence efficiency, λ_C, is employed in the model to depict the randomness of the coalescence phenomenon after each collision. Nevertheless, the constant coalescence efficiency is only an approximation and further efforts are needed to model the efficiency mechanistically. The mean-bubble fluctuation velocity, u_t, in Eq.(11-69) is proportional to the root-mean-square liquid fluctuating velocity difference between two points of length scale, D_b, and is given by $\varepsilon^{1/3} D_b^{1/3}$ where ε is the energy dissipation rate per unit mass of the continuous medium (Rotta, 1972). Thus, the decrease rate of the interfacial area concentration due to the bubble coalescence caused by random collisions, ϕ_{RC}, is given by

$$\begin{aligned}\phi_{RC} &= -\frac{1}{3\psi}\left(\frac{\alpha_g}{a_i}\right)^2 f_{RC} n_b \lambda_C \\ &= -\frac{\Gamma_{RC}\alpha_g^2 \varepsilon^{1/3}}{D_b^{5/3}}\left\{\frac{1}{\alpha_{g,max}^{1/3}\left(\alpha_{g,max}^{1/3}-\alpha_g^{1/3}\right)}\right\} \\ &\times\left\{1-\exp\left(-C_T\frac{\alpha_{g,max}^{1/3}\alpha_g^{1/3}}{\alpha_{g,max}^{1/3}-\alpha_g^{1/3}}\right)\right\}\end{aligned} \tag{11-70}$$

where Γ_{RC} is an adjustable parameter depending on the properties of the fluid, which is determined experimentally to be 0.016. The constants in Eq.(11-70) are set at $\alpha_{g,max}$=0.75 and C_T=3.

B. Bubble coalescence due to wake entrainment

When bubbles enter the wake region of a leading bubble, they will accelerate and may collide with the preceding one (Otake et al., 1977; Bilicki and Kestin, 1987; Stewart, 1995). For a spherical bubble with attached wake region in the liquid medium, the effective wake volume, V_W, in which the following bubbles may collide with the leading one, is defined

as the projected bubble area multiplied by the effective length, L_W. The number of bubbles inside the effective volume, N_W, is then given by

$$N_W = V_W n_b \approx \frac{1}{4}\pi D_b^2 \left(L_W - \frac{D_b}{2}\right) n_b. \tag{11-71}$$

Assuming that the average time interval for a bubble in the wake region to catch up with the preceding bubble is Δt_W, the collision rate per unit mixture volume, R_{WE}, should satisfy

$$\begin{aligned} R_{WE} &\propto \frac{1}{2} n_b \frac{N_W}{\Delta t_W} \approx \frac{1}{8}\pi D_b^2 n_b^2 \left(\frac{L_W - D_b/2}{\Delta t_W}\right) \\ &\approx \frac{1}{8}\pi D_b^2 n_b^2 u_{rW}. \end{aligned} \tag{11-72}$$

where u_{rW} is the averaged relative velocity between the leading bubble and the bubble in the wake region. Schlichting (1979) gave the analytical expression of non-dimensionalized relative velocity as

$$\frac{v_{rW}}{v_r} \approx \left(\frac{C_D A}{\beta^2 y^2}\right)^{1/3} \tag{11-73}$$

where v_{rW}, v_r, C_D, A, β and y are: the relative velocity between the leading bubble and the bubble in the wake region; the relative velocity between the leading bubble and the liquid phase; the drag coefficient; the frontal area of the bubble; the ratio of the mixing length and the width of the wake; and the distance along the flow direction measured from the center of the leading bubble. The averaged relative velocity in the wake region, u_{rW}, is then obtained by integrating v_{rW} over the critical distance as

$$\begin{aligned} u_{rW} &\approx 3 v_{rW} \left(\frac{C_D \pi}{\beta^2}\right)^{1/3} \frac{1}{L_W/\left(D_b/2\right) - 1} \left\{ \left(\frac{L_W}{D_b/2}\right)^{1/3} - 1 \right\} \\ &\approx F\left(\frac{L_W}{D_b}\right) C_D^{1/3} v_r \end{aligned} \tag{11-74}$$

where $F\left(L_W/D_b\right)$ is a function of L_W/D_b, since β is usually assumed to be constant (Schlichting, 1979). The exact form of $F\left(L_W/D_b\right)$ is not important

since the effective bubble wake region may not be fully established. According to Tsuchiya et al. (1989), the wake length is roughly 5-7 times the bubble diameter in an air-water system, and thus L_W/D_b as well as $F\left(L_W/D_b\right)$ are treated as constants depending on the fluid properties. As long as their values obtained from experimental data fall into the range of L_W/D_b =5-7, the mechanism should be acceptable. Thus, the decrease rate of the interfacial area concentration due to the bubble coalescence caused by wake entrainment, ϕ_{WE}, is given by

$$\phi_{WE} = -\frac{1}{3\psi}\left(\frac{\alpha_g}{a_i}\right)^2 R_{WE}\lambda_C = -\frac{\Gamma_{WE}C_D^{1/3}\alpha_g^2 v_r}{D_b^2}. \tag{11-75}$$

where Γ_{WE} is an adjustable parameter mainly determined by the ratio of the effective wake length to the bubble size and the coalescence efficiency, which is determined experimentally to be 0.0076.

C. Bubble breakup due to turbulent impact

For binary bubble breakup due to the impact of turbulent eddies, the driving force comes from the inertial force, $F_{inertia}$, of the turbulent eddies in the continuous medium, while the holding force is the surface tension force, $F_{tension}$. To drive the daughter bubbles apart with a characteristic length of D_b within time interval Δt_B, a simple momentum balance approach gives the following relation.

$$\frac{\rho_f D_b^3 D_b}{\Delta t_B^2} \propto F_{inertia} - F_{tension} \tag{11-76}$$

Here, the inertia of the bubble is dominated by the virtual mass because of the large density ratio of the liquid and gas. Rearranging Eq.(11-76) leads to the following averaged bubble breakup frequency

$$f_{TI} \propto \frac{u_t}{D_b}\left(1-\frac{We_{crit}}{We}\right)^{1/2},\ We \equiv \frac{\rho_f u_t^2 D_b}{\sigma} > We_{crit}. \tag{11-77}$$

The velocity, u_t, is assumed to be the root-mean-square velocity difference between two points of length D_b, which implies that only the eddies with sizes equivalent to the bubble size can break the bubble. We_{crit} is a collective constant, designated as a critical Weber number. The reported value of We_{crit} for bubble breakup varies in a wide range due to the resonance excitation of the turbulent fluctuation (Sevik and Park, 1973).

In a homogeneous turbulent flow, the probability for a bubble to collide with an eddy that has sufficient energy to break the bubble, namely the breakup efficiency, λ_B, is approximately (Coulaloglou and Tavlarrides, 1976)

$$\lambda_B \propto \exp\left(-\frac{u_{t,crit}^2}{u_t^2}\right) \tag{11-78}$$

where $u_{t,crit}^2$ is the critical mean-square fluctuation velocity obtained from We_{crit}. Finally, the increase rate of the interfacial area concentration due to the bubble breakup caused by turbulent impact, ϕ_{TI}, is given by

$$\begin{aligned}\phi_{TI} &= \frac{1}{3\psi}\left(\frac{\alpha_g}{a_i}\right)^2 f_{TI} n_b \lambda_B \\ &= \begin{cases} \dfrac{\Gamma_{TI}\alpha_g \varepsilon^{1/3}}{D_b^{5/3}}\left(1-\dfrac{We_{crit}}{We}\right)^{1/2}\exp\left(-\dfrac{We_{crit}}{We}\right), & We > We_{crit} \\ 0, \; We \le We_{crit}. \end{cases}\end{aligned} \tag{11-79}$$

The adjustable parameters Γ_{TI} and We_{crit} are determined experimentally to be 0.17 and 6.0, respectively. This expression differs from the previous models (Prince and Blanch, 1990) because the breakup rate equals zero when the Weber number is less than We_{crit}. This unique feature permits the decoupling of the bubble coalescence and breakup processes. At a low liquid flow rate with small void fraction, the turbulent fluctuation is small and thus no breakup would be counted. This allows the fine-tuning of the adjustable parameters in the coalescence terms, independent of the bubble breakage.

D. One-dimensional one-group model

The simplest form of the interfacial area transport equation is the one-dimensional formulation obtained by applying cross-sectional area averaging over Eq.(11-60)

$$\begin{aligned}&\frac{\partial\langle a_i\rangle}{\partial t}+\frac{\partial}{\partial z}\left(\langle a_i\rangle\langle\langle v_{i,z}\rangle\rangle_a\right)=\left(\langle\phi_{RC}\rangle+\langle\phi_{WE}\rangle+\langle\phi_{TI}\rangle\right) \\ &+\frac{2}{3}\left(\frac{\langle a_i\rangle}{\langle\alpha_g\rangle}\right)\left[\frac{\partial\langle\alpha_g\rangle}{\partial t}+\frac{\partial}{\partial z}\left(\langle\alpha_g\rangle\langle\langle v_{g,z}\rangle\rangle\right)\right].\end{aligned} \tag{11-80}$$

Due to the uniform bubble size assumption, the area-averaged bubble interface velocity weighted by interfacial area concentration, $\left\langle\left\langle v_{i,z}\right\rangle\right\rangle_a$, is given by

$$\left\langle\left\langle v_{i,z}\right\rangle\right\rangle_a \equiv \frac{\left\langle a_i v_{i,z}\right\rangle}{\left\langle a_i\right\rangle} \approx \frac{\left\langle \alpha_g v_{g,z}\right\rangle}{\left\langle \alpha_g\right\rangle} \equiv \left\langle\left\langle v_{g,z}\right\rangle\right\rangle. \tag{11-81}$$

This is the same as the conventional area-averaged gas velocity weighted by void fraction, if the internal circulation in the bubble is neglected. The exact mathematical expressions for the area-averaged source and sink terms would involve many covariances that may further complicate the one-dimensional problem. However, since these local terms were originally obtained from a finite volume element of the mixture, the functional dependence of the area-averaged source and sink terms on the averaged parameters should be approximately the same if the hydraulic diameter of the flow path is considered as the length scale of the finite element. Therefore, Eqs.(11-70), (11-75) and (11-79), with the parameters averaged within the cross-sectional area, are still applicable for the area-averaged source and sink terms in Eq.(11-80).

In Eqs.(11-70), (11-75) and (11-79), the energy dissipation rate per unit mixture mass should be specified. In a complete two-fluid model, ε comes from its own constitutive relation such as the two-phase k-ε model (Lopez de Bertodano et al., 1994). For one-dimensional analysis, however, this term can be approximated by a simple algebraic equation as

$$\langle\varepsilon\rangle = \frac{f_{TW}}{2D_H}\left\langle v_m\right\rangle^3 \tag{11-82}$$

where v_m, D_H and f_{TW} are the mean mixture velocity, the hydraulic diameter of the flow path and the two-phase friction factor.

1.2.2 Source and sink terms modeled by Hibiki and Ishii (2000a)

Hibiki and Ishii (2000a; 2002c) discussed the contribution of wake entrainment to the interfacial area transport. Wake entrainment would play an important role in the bubbly-to-slug transition, slug and churn-turbulent flows. It may also be important for bubbly flow in a small diameter tube or for very low flow conditions as the lateral fluctuation of bubbles is small. However, for relatively high flow conditions, even bubbles captured in the wake region would easily leave the wake region due to liquid turbulence, resulting in a minor contribution of wake entrainment to the interfacial area

transport. Thus, Hibiki and Ishii (2000a) dropped the wake entrainment term from the interfacial area transport equation in an adiabatic bubbly flow, and considered two terms of coalescence due to random collisions driven by liquid turbulence and breakup due to the impact of turbulent eddies.

A. Bubble coalescence due to random collision

The bubble coalescence is considered to occur due to the bubble random collision induced by turbulence in a liquid phase. For the estimation of bubble-bubble collision frequency, it is assumed that the movement of bubbles behaves like ideal gas molecules (Coulaloglou and Tavlarides, 1977). Following the kinetic theory of gases (Loeb, 1927), the bubble random collision frequency, f_{RC}, can be expressed by assuming the same velocity of bubbles, u_C, as a function of surface available to the collision, S_C, and volume available to the collision, U_C

$$f_{RC} = \frac{u_C S_C}{4U_C}. \tag{11-83}$$

Taking account of the excluded volume for bubbles, the surface and volume are given by

$$S_C = 4\pi\left(N_b - 1\right)D_b^2 \cong 4\pi N_b D_b^2 = V\frac{24\alpha_g}{D_b} \tag{11-84}$$

$$\begin{aligned} U_C &= V\left(1 - \beta_C \frac{2}{3}\pi n_b D_b^3\right) \\ &= 4\beta_C V\left(\alpha_{C,max} - \alpha_g\right),\ \alpha_{C,max} \equiv 1/4\beta_C \end{aligned} \tag{11-85}$$

where N_b, D_b, V, n_b and α_g denote the number of bubbles, the bubble diameter, the control volume, the bubble number density and the void fraction, respectively. The variable β_C (≤ 1) is introduced into the excluded volume in order to take account of the overlap of the excluded volume for high void fraction region. Although it may be a function of the void fraction, it is treated as a constant for simplicity. The distortion caused by this assumption will be adjusted by a tuning parameter in a final equation of the bubble coalescence rate as introduced later.

The mean fluctuation velocity difference between two points D_b in the inertial subrange of isotropic turbulence is given by (Hinze, 1959)

$$u_b = 1.4(\varepsilon D_b)^{1/3} \tag{11-86}$$

where ε denotes the energy dissipation. Taking account of the relative motion between bubbles, the average bubble velocity is given by

$$u_C = \gamma_C (\varepsilon D_b)^{1/3} \tag{11-87}$$

where γ_C is a constant.

The collision frequency will increase to infinity as the void fraction approaches to maximum void fraction, $\alpha_{C,max}$. Since 74.1 % of the volume is actually occupied by identical spheres close-packed according to a face-centered cubic lattice, $\alpha_{C,max}$ may be assumed to be 0.741. Finally, we obtain

$$f_{RC} = \frac{\gamma_C' \alpha_g \varepsilon^{1/3}}{D_b^{2/3}(\alpha_{C,max} - \alpha_g)} \tag{11-88}$$

where γ_C' is an adjustable valuable.

In order to obtain the bubble coalescence rate, it is necessary to determine a coalescence efficiency. Coulaloglou and Tavlarides (1977) gave an expression for the coalescence efficiency, λ_C, as a function of a time required for coalescence of bubbles, t_C, and a contact time for the two bubbles τ_C

$$\lambda_C = \exp\left(-\frac{t_C}{\tau_C}\right). \tag{11-89}$$

The time required for coalescence of bubbles was given by Oolman and Blanch (1986a; 1986b) for the thinning of the liquid film between bubbles of equal size as

$$t_C = \frac{1}{8}\sqrt{\frac{\rho_f D_b^3}{2\sigma}} \ln\frac{\delta_{init}}{\delta_{crit}} \tag{11-90}$$

where ρ_f, σ, δ_{init} and δ_{crit} are, respectively, the liquid density, interfacial tension, the initial film thickness, and the critical film thickness where rupture occurs. Levich (1962) derived the contact time in turbulent flows from dimensional consideration.

$$\tau_C = \frac{r_b^{2/3}}{\varepsilon^{1/3}} \tag{11-91}$$

where r_b is the bubble radius. Finally, we obtain

$$\lambda_C = \exp\left(-\frac{K_C \rho_f^{1/2} D_b^{5/6} \varepsilon^{1/3}}{\sigma^{1/2}}\right) \text{ where } K_C \equiv 2^{-17/6} \ln\frac{\delta_{init}}{\delta_{crit}}. \tag{11-92}$$

Kirkpatrick and Locket (1974) estimated the initial thickness of the film in air-water systems to be 1×10^{-4} m, whereas the final film thickness was typically taken as 1×10^{-8} m (Kim and Lee, 1987). Thus, the experimental coefficient, K_C, is determined to be 1.29 for an air-water system.

The decrease rate of the interfacial area concentration, ϕ_{RC}, is then expressed as

$$\begin{aligned}\phi_{RC} &= -\frac{1}{3\psi}\left(\frac{\alpha_g}{a_i}\right)^2 f_{RC} n_b \lambda_C \\ &= -\frac{\Gamma_{RC}\alpha_g^2 \varepsilon^{1/3}}{D_b^{5/3}\left(\alpha_{C,\max} - \alpha_g\right)} \exp\left(-\frac{K_C \rho_f^{1/2} D_b^{5/6} \varepsilon^{1/3}}{\sigma^{1/2}}\right).\end{aligned} \tag{11-93}$$

The adjustable variable, Γ_{RC}, would certainly be a function of the overlap of the excluded volume, the bubble deformation, and the bubble velocity distribution. However, the adjustable variable might be assumed to be a constant for simplicity and is determined experimentally to be 0.0314 for bubbly flow.

B. Bubble breakup due to turbulent impact

The bubble breakup is considered to occur due to the collision of the turbulent eddy with the bubble. For the estimation of bubble-eddy collision frequency, it is assumed that the movement of eddies and bubbles behaves like ideal gas molecules (Coulaloglou and Tavlarides, 1977). Furthermore, the following assumptions are made for the modeling of the bubble-eddy collision rate (Prince and Blanch, 1990): (i) the turbulence is isotropic; (ii) the eddy size D_e of interest lies in the inertial subrange; (iii) the eddy with the size from $c_e D_b$ to D_b can break up the bubble with the size of D_b, since larger eddies have the tendency to transport the bubble rather than to break it and smaller eddies do not have enough energy to break it. Azbel and

Athanasios (1983) developed the following expression for the number of eddies as a function of wave number.

$$\frac{dN_e(k_e)}{dk_e} = 0.1k_e^2 \tag{11-94}$$

where $N_e(k_e)$ denotes the number of eddies of wave number $k_e (=2/D_e)$ per volume of fluid. Here, the number of eddies of wave number per volume of two-phase mixture, $n_e(k_e)$, is given by

$$n_e(k_e) = N_e(k_e)(1-\alpha_g). \tag{11-95}$$

Following the kinetic theory of gases (Loeb, 1927), the bubble-eddy random collision frequency, f_{TI}, can be expressed by assuming the same velocity of bubbles, u_B, as a function of the surface available to the collision, S_B, and the volume available to the collision U_B

$$f_{TI} = \frac{u_B S_B}{4U_B}. \tag{11-96}$$

Taking account of the excluded volume for the bubbles and eddies, the surface and volume are given by

$$\begin{aligned} S_B &= \frac{\int 4\pi(N_b - 1)\left(\frac{D_b}{2} + \frac{D_e}{2}\right)^2 dn_e}{\int dn_e} \\ &= 4\pi N_b D_b^2 \cdot F_S(c_e) = V\frac{24\alpha_g}{D_b}F_S(c_e) \end{aligned} \tag{11-97}$$

$$\begin{aligned} U_B &= V\left(1 - \frac{\beta_B \int \frac{2}{3}\pi n_b \left(\frac{D_b}{2} + \frac{D_e}{2}\right)^3 dn_e}{\int dn_e}\right) \\ &= V\left(1 - \beta_B \frac{2}{3}\pi n_b D_b^3 \cdot F_V(c_e)\right) \end{aligned} \tag{11-98}$$

$$= 4\beta_B F_V(c_e) V\left(\alpha_{B,max} - \alpha_g\right)$$

where $F_S(c_e)$ and $F_V(c_e)$ are functions of c_e defined by D_e/D_b. The variable β_B (≤ 1) is introduced into the excluded volume in order to take account of the overlap of the excluded volume for high void fraction region. Although it may be a function of the void fraction, it is treated as a constant for simplicity. The distortion caused by this assumption will be adjusted by a tuning parameter in a final equation of the bubble breakup rate as introduced later.

According to Kolmogorov's Law (Azbel, 1981), for the inertial subrange of the energy spectrum, the eddy velocity, u_e, is given as

$$u_e^2 = 8.2\left(\varepsilon/k_e\right)^{2/3} \quad \text{or} \quad u_e = 2.3(\varepsilon D_e)^{1/3}. \tag{11-99}$$

Here, taking account of the relative motion between bubble and eddy, the averaged relative velocity, u_B, can be expressed as

$$u_B = \gamma_B(c_e)(\varepsilon D_b)^{1/3} \tag{11-100}$$

where $\gamma_B(c_e)$ is a function of c_e. Finally, we obtain

$$f_B = \frac{\gamma_B'(c_e)\alpha_g \varepsilon^{1/3}}{D_b^{2/3}\left(\alpha_{B,max} - \alpha_g\right)} \tag{11-101}$$

where $\gamma_B'(c_e)$ and $\alpha_{B,max}$ are an adjustable variable depending on c_e and maximum allowable void fraction, respectively. The maximum allowable void fraction, $\alpha_{B,max}$, in Eq.(11-101) can approximately be taken at the same value as $\alpha_{C,max}$, namely, 0.741, if eddies with almost the same size of bubbles are assumed to break up the bubbles. Consequently, the functional form of the frequency of the bubble-eddy random collision, Eq.(11-101) looks similar to that of the frequency of the bubble-bubble random collision, Eq.(11-88).

In order to obtain the bubble breakup rate, it is necessary to determine a breakup efficiency, λ_B. The breakup efficiency is given in terms of the average energy of a single eddy, E_e, and the average energy required for bubble breakup, E_B, as (Prince and Blanch, 1990; Coulaloglou and Tavlarides, 1977; Tsouris and Tavlarides, 1994)

$$\lambda_B = \exp\left(-\frac{E_B}{E_e}\right). \tag{11-102}$$

For binary breakage, that is, the bubble breaks into two bubbles, the required energy, E_B, is simply calculated as the average value of the energy required for breakage into a small and a large daughter bubble as follows

$$E_B = \pi\sigma D_{b,\max}^2 + \pi\sigma D_{b,\min}^2 - \pi\sigma D_b^2. \tag{11-103}$$

The average values of the breakup energy for two extreme cases are calculated by averaging Eq.(11-103) from $D_{b,max} = D_b/2^{1/3}$ ($D_{b,min} = D_b/2^{1/3}$) to $D_{b,max} = D_b$ ($D_{b,min} = 0$) to be $0.200\pi\sigma D_b^2$ and by setting $D_{b,max} = D_{b,min} = D_b/2^{1/3}$ to be $0.260\pi\sigma D_b^2$. Thus, the breakup energy, E_B, is approximated to be $0.230\pi\sigma D_b^2$ by averaging the breakup energies for two extreme cases. It should be noted here that the relative difference between E_B ($= 0.230\pi\sigma D_b^2$) obtained by averaging Eq.(11-103) and E_B ($= 0.260\pi\sigma D_b^2$) assuming the binary breakage into two equal-size bubbles is about 13 %. Therefore, the assumption on the size of small and large daughter bubbles may not affect the estimation of E_B significantly.

The average energy of single eddies acting on the bubble breakup is simply calculated from

$$E_e = \frac{\int_{n_{e,\min}}^{n_{e,\max}} e dn_e}{\int_{n_{e,\min}}^{n_{e,\max}} dn_e} \tag{11-104}$$

where e is the energy of a single eddy given by

$$e = \frac{1}{2} m_e u_e^2. \tag{11-105}$$

In this, m_e is the mass per a single eddy. From Eqs.(11-94), (11-95), (11-99), (11-104) and (11-105), the average energy of single eddies acting on the bubble breakup is then given by

$$E_e = \frac{\int_{n_{e,\min}}^{n_{e,\max}} e dn_e}{\int_{n_{e,\min}}^{n_{e,\max}} dn_e} = \frac{0.546\pi\rho_f\varepsilon^{2/3}(1-\alpha_g)\int_{k_{e,\min}}^{k_{e,\max}} k_e^{-5/3} dk_e}{0.1(1-\alpha_g)\int_{k_{e,\min}}^{k_{e,\max}} k_e^2 dk_e} \tag{11-106}$$

$$= 1.93\pi\rho_f\varepsilon^{2/3}D_b^{11/3}\frac{1-c_e^{2/3}}{c_e^{-3}-1}.$$

Prince and Blanch (1990) set the minimum eddy size, which would not cause bubble breakup, at eddies smaller than 20 % of the bubble size, c_e^3=0.2. Thus, the average energy of single eddies is expressed by

$$E_e = 0.145\pi\rho_f\varepsilon^{2/3}D_b^{11/3}. \tag{11-107}$$

The final form of the breakup efficiency is then given by

$$\lambda_B = \exp\left(-\frac{K_B\sigma}{\rho_f D_b^{5/3}\varepsilon^{2/3}}\right) \tag{11-108}$$

where K_B is a constant to be 1.59 (=0.230/0.145).

The increase rate of the interfacial area concentration, ϕ_{TI}, is then expressed as

$$\phi_{TI} = \frac{1}{3\psi}\left(\frac{\alpha_g}{a_i}\right)^2 f_{TI} n_e \lambda_B$$
$$= \frac{\Gamma_B\alpha_g(1-\alpha_g)\varepsilon^{1/3}}{D_b^{5/3}(\alpha_{B,\max}-\alpha_g)}\exp\left(-\frac{K_B\sigma}{\rho_f D_b^{5/3}\varepsilon^{2/3}}\right) \tag{11-109}$$

where Γ_{TI} is an adjustable variable. The adjustable variable, Γ_B, would certainly be a function of the overlap of the excluded volume, the bubble deformation, the bubble velocity distribution, and the ratio of eddy size to bubble size. However, the adjustable variable might be assumed to be a constant for simplicity and is determined experimentally to be 0.0209 for bubbly flow.

It should be noted here that for one-dimensional analysis the energy dissipation rate per unit mass is simply obtained from the mechanical energy equation (Bello, 1968) as

$$\langle \varepsilon \rangle = \frac{\langle j \rangle}{\rho_m} \left(-\frac{dP}{dz} \right)_F \tag{11-110}$$

where j, ρ_m, P and z denote the mixture volumetric flux, the mixture density, the pressure, and the axial position from the test section inlet, respectively.

1.2.3 Source and sink terms modeled by Hibiki et al. (2001b)

Hibiki et al. (2001b) discussed the main mechanism of the interfacial area transport in a relatively small diameter tube at low liquid velocity where the bubble breakup is negligible. Here, a relatively small diameter tube is defined as a tube with a relatively high bubble size-to-pipe diameter ratio. In such a relatively small diameter tube, the radial bubble movement would be restricted due to the presence of the wall resulting in insignificant bubble random collision, whereas the bubbles are aligned along the flow direction resulting in significant wake entrainment. Thus, Hibiki et al. (2001b) developed the sink term due to the bubble coalescence considering the dependence of the bubble coalescence mechanism on the tube diameter.

A. Bubble coalescence due to random collision

The same model as in Hibiki and Ishii (2000a) was used.

$$\phi_{RC} = -\frac{\Gamma_{RC} \alpha_g^2 \varepsilon^{1/3}}{D_b^{5/3} \left(\alpha_{C,\max} - \alpha_g \right)} \exp\left(-\frac{K_C \rho_f^{1/2} D_b^{5/6} \varepsilon^{1/3}}{\sigma^{1/2}} \right) \tag{11-111}$$

B. Bubble coalescence due to wake entrainment

The model was developed by modifying the model proposed by Wu et al. (1998).

$$\phi_{WE} = -\Gamma_{WE} C_D^{1/3} a_i^2 v_r \exp\left(-\frac{K_C \rho_f^{1/2} D_b^{5/6} \varepsilon^{1/3}}{\sigma^{1/2}} \right) \tag{11-112}$$

where Γ_{WE} and K_C are, respectively, an adjustable parameter experimentally determined to be 0.082 and the experimental constant determined to be 1.29 for an air-water system.

C. Effect of tube size on interfacial area transport mechanism

The above simple consideration suggests that the major mechanism of the

bubble coalescence in a relatively small diameter tube would be wake entrainment. However, experimental data (Hibiki and Ishii, 1999; Hibiki et al., 2001a) suggested that the bubble coalescence mechanism of bubbly flows in medium pipes (25.4 mm $\leq D \leq$ 50.8 mm) could successfully be modeled by considering the bubble random collision induced by liquid turbulence. Thus, the bubble coalescence mechanism is likely to be dependent on the ratio of bubble diameter to tube diameter, D_b/D. For example, a trailing bubble should certainly exist in a projected area of a leading bubble for D_b/D=0.5. Also, if the leading bubble rises in the center of the channel, the trailing bubble should certainly exist in the projected area of the leading bubble even for D_b/D=0.33. In a small diameter tube, since the radial bubble movement would be restricted due to the presence of the wall, the bubble coalescence due to bubble random collision is unlikely to occur. Thus, as the ratio of bubble diameter to tube diameter increases, the dominant bubble coalescence mechanism is expected to change from the bubble random collision to the wake entrainment. This suggests the following functional form of the sink term for bubbly flows in small and medium tubes.

$$\phi_C = \phi_{RC} \exp\left\{f\left(\frac{D_b}{D}\right)\right\} + \phi_{WE}\left[1 - \exp\left\{f\left(\frac{D_b}{D}\right)\right\}\right] \tag{11-113}$$

The function, $f\left(D_b/D\right)$, may be approximated based on experimental data as

$$f\left(\frac{D_b}{D}\right) = -1000\left(\frac{D_b}{D}\right)^5. \tag{11-114}$$

The interfacial area transport equation taking account of the tube size effect would be promising for predicting the interfacial area transport of bubbly flows in small and medium tubes.

1.3 Modeling of source and sink terms in two-group interfacial area transport equation

The interfacial structures in different flow regimes change dramatically. For cap bubbly, slug and churn-turbulent flows, bubbles are divided into two groups according to their geometrical and physical characteristics. The spherical and distorted bubbles are categorized as Group 1, and the cap, slug and churn-turbulent bubbles are categorized as Group 2. These two groups are subject to different coalescence/disintegration mechanisms. Therefore, a

two-group interfacial area transport equation needs to be introduced and the bubble coalescence and breakup processes should be modeled properly. In this section, some two-group models are explained briefly.

1.3.1 Source and sink terms modeled by Hibiki and Ishii (2000b)

Hibiki and Ishii (2000b) developed the two-group interfacial area transport equation at adiabatic bubbly-to-slug transition flow in a moderate diameter tube and evaluated it using a vertical air-water flow data taken in a 50.8 mm-diameter tube (Hibiki et al., 2001a). In what follows, the classification of interfacial area transport mechanisms and the modeled source and sink terms are explained briefly.

A. Classification of interfacial area transport mechanisms

The boundary between Group-1 and Group-2 bubbles can be determined by (Ishii and Zuber, 1979)

$$D_{crit} = 4\sqrt{\frac{\sigma}{g\Delta\rho}} \tag{11-115}$$

where D_{crit} is the volumetric equivalent diameter of a bubble at the boundary between Group-1 and Group-2 bubbles. Equation (11-115) gives the value of about 10 mm for air-water system at atmospheric pressure.

To model the integral source and sink terms in two-group interfacial area transport equation caused by bubble coalescence and breakup, the possible combinations of bubble interactions can be classified into eight categories in terms of the belonging bubble group (see Fig.11-1): (1) the coalescence of bubbles (Group 1) into a bubble (Group 1); (2) the breakup of a bubble (Group 1) into bubbles (Group 1); (3) the coalescence of bubbles (Group 1 and 2) into a bubble (Group 2); (4) the breakup of a bubble (Group 2) into bubbles (Group 1 and 2); (5) the coalescence of bubbles (Group 1) into a bubble (Group 2); (6) the breakup of a bubble (Group 2) into bubbles (Group 1); (7) the coalescence of bubbles (Group 2) into a bubble (Group 2); and (8) the breakup of a bubble (Group 2) into bubbles (Group 2). As summarized in Table 11-1, Hibiki and Ishii (2000b) considered the three major bubble interactions: (1) the coalescence due to random collisions driven by turbulence; (2) the coalescence due to wake entrainment; and (3) the breakup upon the impact of turbulent eddies. They assumed that the bubble coalescence due to the shearing-off of cap or slug bubbles might be insignificant at bubbly-to-slug transition flow. They also assumed the bubble breakup due to surface instability could be neglected in a moderate

Table 11-1. List of intra- and inter-group interaction mechanisms in the model by Hibiki and Ishii (2000b)

Symbols	Mechanisms	Interaction	Parameters
$\phi_{RC}^{(1)}$	Random collision	(1)+(1)→(1)	$\Gamma_{RC,1}$=0.351, $K_{RC,1}$=0.258
$\phi_{WE}^{(12,2)}$	Wake entrainment	(1)+(2)→(1)	$\Gamma_{WE,12}$=24.9, $K_{WE,12}$=0.460
$\phi_{WE}^{(2)}$	Wake entrainment	(2)+(2)→(2)	$\Gamma_{WE,2}$=63.7, $K_{WE,2}$=0.258
$\phi_{TI}^{(1)}$	Turbulent impact	(1)→(1)+(1)	$\Gamma_{TI,1}$=1.12, $K_{TI,1}$=6.85
$\phi_{TI}^{(2)}$	Turbulent impact	(2)→(2)+(1)	$\Gamma_{TI,12}$=317, $K_{TI,12}$=11.7
$\phi_{TI}^{(2,12)}$	Turbulent impact	(2)→(2)+(2)	$\Gamma_{TI,2}$=4.26, $K_{TI,2}$=6.85

diameter tube where the tube size is smaller than the limit of the bubble breakup due to surface instability.

Hibiki and Ishii (2000b) developed the two-group model with the necessary inter-group coupling terms due to turbulent impact and wake entrainment as well as source and sink terms due to wake entrainment and turbulent impact in Group 2 (see Table 11-1). Here, some other mechanisms such as coalescence due to random collision between cap bubbles are excluded because the model is developed for bubbly-to-slug transition flow in a moderate diameter tube. In such a condition, cap and slug bubbles would rise around the tube center resulting in a minor role of random collision between cap bubbles. Two more mechanisms are also omitted in this model. They are interchange terms due to the complete breakup of a cap bubble (Group 2) into small bubbles (Group 1) and the coalescence of small bubbles (Group 1) into a cap bubble (Group 2). Since the ratio in diameter of cap bubbles to small bubbles is about 10 to 20 in the experimental conditions of the database (Hibiki et al., 2001a), these interchanges of bubbles are unlikely to occur. Eventually, six terms listed in Table 11-1 are considered as source and sink terms in the two-group interfacial area transport equations to be applied at the bubbly-to-slug transition flow in a moderate diameter tube.

B. Simplified two-group interfacial area transport equation

Here, an isothermal flow condition is assumed. In addition, the coefficient χ is neglected. It is due to the fact that there is very little portion of bubbles at the group boundary that could transfer to the other group simply due to expansion. Thus, two-group interfacial area transport equation is simplified as

$$\frac{\partial\left(\alpha_{g1}\rho_g\right)}{\partial t}+\nabla\cdot\left(\alpha_{g1}\rho_g\boldsymbol{v}_{g1}\right)=-\rho_g\left(\eta_{WE}^{(12,2)}+\eta_{TI}^{(2,12)}\right) \tag{11-116}$$

$$\frac{\partial a_{i1}}{\partial t}+\nabla\cdot\left(a_{i1}\boldsymbol{v}_{i1}\right)=\frac{2}{3}\frac{a_{i1}}{\alpha_{g1}}\left[\frac{\partial\alpha_{g1}}{\partial t}+\nabla\cdot\left(\alpha_{g1}\boldsymbol{v}_{g1}\right)\right] \tag{11-117}$$
$$+\phi_{RC}^{(1)}+\phi_{WE}^{(12,2)}+\phi_{TI}^{(1)}+\phi_{TI}^{(2,12)}$$

$$\frac{\partial a_{i2}}{\partial t}+\nabla\cdot\left(a_{i2}\boldsymbol{v}_{i2}\right)=\frac{2}{3}\frac{a_{i2}}{\alpha_{g2}}\left[\frac{\partial\alpha_{g2}}{\partial t}+\nabla\cdot\left(\alpha_{g2}\boldsymbol{v}_{g2}\right)\right] \tag{11-118}$$
$$+\phi_{WE}^{(2)}+\phi_{TI}^{(2)}.$$

C. Summary of modeled sink and source terms

The modeled sink and source terms are summarized as follows. In the one-dimensional formulation, all the two-phase parameters, such as α_g, a_i, and D_{Sm}, are area-averaged values. For simplicity, the $\langle\ \rangle$ signs standing for the area-average are omitted in the following formulations.

Bubble coalescence due to random collision

$$\phi_{RC}^{(1)}=-\frac{\Gamma_{RC,1}\alpha_{g1}^2\varepsilon^{1/3}}{D_{b,1}^{5/3}\left(\alpha_{C,\max}-\alpha_g\right)}\exp\left(-\frac{K_{RC,1}\rho_f^{1/2}D_{b,1}^{5/6}\varepsilon^{1/3}}{\sigma^{1/2}}\right) \tag{11-119}$$

Bubble coalescence due to wake entrainment

$$\phi_{WE}^{(12,2)}=-\frac{\Gamma_{WE,12}\alpha_{g1}\alpha_{g2}}{D_{b,1}D_{b,2}}\left(v_{g2}-v_f\right)$$
$$\times\exp\left\{-K_{WE,12}\sqrt[6]{\frac{\rho_f^3\varepsilon^2}{\sigma^3}\left(\frac{D_{b,1}D_{b,2}}{D_{b,1}+D_{b,2}}\right)^5}\right\} \tag{11-120}$$

$$\phi_{WE}^{(2)} = -\frac{\Gamma_{WE,2}\alpha_{g2}^2}{D_{b,2}^2}\left(v_{g2} - v_f\right)\exp\left\{-K_{WE,2}\sqrt[6]{\frac{D_{b,2}^5\rho_f^3\varepsilon^2}{\sigma^3}}\right\} \tag{11-121}$$

$$\eta_{WE}^{(12,2)} = \left(\frac{\alpha_{g1}}{a_{i,1}}\right)^3 \frac{3\Gamma_{WE,12}\alpha_{g1}\alpha_{g2}}{D_{b,1}^3 D_{b,2}}\left(v_{z,2} - v_f\right)$$
$$\times\exp\left\{-K_{WE,12}\sqrt[6]{\frac{\rho_f^3\varepsilon^2}{\sigma^3}\left(\frac{D_{b,1}D_{b,2}}{D_{b,1}+D_{b,2}}\right)^5}\right\} \tag{11-122}$$

Bubble breakup due to turbulent impact

$$\phi_{TI}^{(1)} = \frac{\Gamma_{TI,1}\alpha_{g1}\left(1-\alpha_g\right)\varepsilon^{1/3}}{D_{b,1}^{5/3}\left(\alpha_{TI,\max}-\alpha_g\right)}\exp\left(-\frac{K_{TI,1}\sigma}{\rho_f D_{b,1}^{5/3}\varepsilon^{2/3}}\right) \tag{11-123}$$

$$\phi_{TI}^{(2,12)} = \frac{\Gamma_{TI,12}\alpha_{g2}\left(1-\alpha_g\right)\varepsilon^{1/3}}{D_{b,2}^{5/3}\left(\alpha_{TI,\max}-\alpha_g\right)}$$
$$\times\exp\left(-\frac{K_{TI,12}\sigma\left\{\left(D_{b,2}^3 - D_{b,1}^3\right)^{2/3} + \left(D_{b,1}^2 - D_{b,2}^2\right)\right\}}{\rho_f D_{b,2}^{11/3}\varepsilon^{2/3}}\right) \tag{11-124}$$

$$\phi_{TI}^{(2)} = \frac{\Gamma_{TI,2}\alpha_{g2}\left(1-\alpha_g\right)\varepsilon^{1/3}}{D_{b,2}^{5/3}\left(\alpha_{TI,\max}-\alpha_g\right)}\exp\left(-\frac{K_{TI,2}\sigma}{\rho_f D_{b,2}^{5/3}\varepsilon^{2/3}}\right) \tag{11-125}$$

$$\eta_{TI}^{(2,12)} = \left(\frac{\alpha_{g1}}{a_{i,1}}\right)^3 \frac{3\Gamma_{TI,12}\alpha_{g2}\left(1-\alpha_g\right)\varepsilon^{1/3}}{D_{b,2}^{11/3}\left(\alpha_{TI,max}-\alpha_g\right)}$$
$$\times\exp\left(-\frac{K_{TI,12}\sigma\left\{\left(D_{b,2}^3 - D_{b,1}^3\right)^{2/3} + \left(D_{b,1}^2 - D_{b,2}^2\right)\right\}}{\rho_f D_{b,2}^{11/3}\varepsilon^{2/3}}\right) \tag{11-126}$$

The values of the coefficients in the source and sink terms are listed in Table 11-1.

1.3.2 Source and sink terms modeled by Fu and Ishii (2002a)

Fu and Ishii (2002a) developed the two-group interfacial area transport equation for bubbly flow, slug flow, and churn-turbulent flow in a moderate diameter tube and evaluated it using a vertical air-water flow data taken in a 50.8 mm-diameter tube. In what follows, the classification of interfacial area transport mechanisms and the modeled source and sink terms are explained briefly.

A. Classification of interfacial area transport mechanisms

Fu and Ishii (2002a) adopted five major bubble interactions: (1) the coalescence due to random collisions driven by turbulence; (2) the coalescence due to wake entrainment; (3) the breakup upon the impact of turbulent eddies; (4) the breakup due to shearing-off; and (5) the breakup of large-cap bubbles due to flow instability on the bubble surface. In view of the complexity for incorporating all source and sink terms into the interfacial area transport equation and the difficulty of experimental verification, they performed an analysis to simplify the interaction terms according to their nature and the order of magnitudes. It is verified from experiments that the majority of inter-group interactions is caused by the wake entrainment and the shearing-off of Group-1 bubbles to and from the Group-2 bubbles (Fu and Ishii, 2002a). In addition, the wake entrainment between Group-2 bubbles predominantly governs the Group-2 bubble number which significantly affects the flow structure and intensiveness of inter-group interactions. The Group-2 bubble disintegration due to surface instability is significantly enhanced by the high turbulent intensity and active eddy-bubble interaction in the wake region of the slug bubbles.

The random collision between Group-1 and Group-2 bubbles may be included into the wake entrainment of Group-1 into Group-2 bubbles due to the similar nature. In addition, the contribution from the collision of Group-1 bubble at the head of Group-2 bubble could be small due to the lower Group-1 bubble number density and lower turbulent intensity outside the wake region. Meanwhile, the random collision between Group-2 bubbles could also be negligible in a moderate diameter flow (2.5 cm $\leq D \leq$ 10 cm) because the predominant interaction is normally within a wake region of the leading bubble, and the coalescence mechanism can be treated as wake entrainment between Group-2 bubbles. Similarly, the turbulent disintegration that results in a generation of the Group-1 bubble from the Group-2 bubble can be seen as part of the shearing-off effect and might not

Table 11-2. List of intra- and inter-group interaction mechanisms in the model by Fu and Ishii (2002a; 2002b)

Symbols	Mechanisms	Interaction	Parameters
$\phi_{RC}^{(1)}$	Random collision	(1)+(1)→(1)	C_{RC}=0.0041, C_T=3.0
$\phi_{RC}^{(11,2)}$	Random collision	(1)+(1)→(2)	$\alpha_{g1,max}$=0.75
$\phi_{WE}^{(1)}$	Wake entrainment	(1)+(1)→(1)	C_{WE}=0.002, $C_{WE}^{(12,2)}$=0.015
$\phi_{WE}^{(11,2)}$	Wake entrainment	(1)+(1)→(2)	$C_{WE}^{(2)}$=10.0
$\phi_{WE}^{(12,2)}$	Wake entrainment	(1)+(2)→(2)	C_{TI}=0.0085, We_{crit}=6.0
$\phi_{WE}^{(2)}$	Wake entrainment	(2)+(2)→(2)	C_{SO}=0.031, γ_{SO}=0.032
$\phi_{TI}^{(1)}$	Turbulent impact	(1)→(1)+(1)	β_{SO}=1.6
$\phi_{TI}^{(2)}$	Turbulent impact	(2)→(2)+(2)	
$\phi_{SO}^{(2,12)}$	Shearing-off	(2)→(2)+(1)	

need to be modeled individually. Furthermore, the disintegration of Group-2 bubbles due to surface instability is considered to be very small and can be combined with the disintegration of Group-2 bubbles induced by turbulent impact. Eventually, nine terms listed in Table 11-2 are considered as sink and source terms in the two-group interfacial area transport equations to be applied at the bubbly, slug and churn-turbulent flows in a moderate diameter tube.

B. Simplified two-group interfacial area transport equation

Here, an isothermal flow condition is assumed. In addition, the coefficient χ is neglected. It is due to the fact that there is very little portion of bubbles at the group boundary that could transfer to the other group simply due to expansion. Thus, two-group interfacial area transport equation is simplified as

$$\frac{\partial\left(\alpha_{g1}\rho_g\right)}{\partial t}+\nabla\cdot\left(\alpha_{g1}\rho_g\boldsymbol{v}_{g1}\right) = -\rho_g\left(\eta_{RC}^{(11,2)}+\eta_{WE}^{(11,2)}+\eta_{WE}^{(12,2)}+\eta_{SO}^{(2,12)}\right) \tag{11-127}$$

$$\frac{\partial a_{i1}}{\partial t}+\nabla\cdot\left(a_{i1}\boldsymbol{v}_{i1}\right)=\frac{2}{3}\frac{a_{i1}}{\alpha_{g1}}\left[\frac{\partial\alpha_{g1}}{\partial t}+\nabla\cdot\left(\alpha_{g1}\boldsymbol{v}_{g1}\right)\right] \tag{11-128}$$
$$+\phi_{RC}^{(1)}+\phi_{RC,1}^{(11,2)}+\phi_{WE}^{(1)}+\phi_{WE,1}^{(11,2)}+\phi_{WE,1}^{(12,2)}+\phi_{TI}^{(1)}+\phi_{SO,1}^{(2,12)}$$

$$\frac{\partial a_{i2}}{\partial t}+\nabla\cdot\left(a_{i2}\boldsymbol{v}_{i2}\right)=\frac{2}{3}\frac{a_{i2}}{\alpha_{g2}}\left[\frac{\partial\alpha_{g2}}{\partial t}+\nabla\cdot\left(\alpha_{g2}\boldsymbol{v}_{g2}\right)\right] \tag{11-129}$$
$$+\phi_{WE}^{(2)}+\phi_{SO,2}^{(2,12)}+\phi_{RC,2}^{(11,2)}+\phi_{TI}^{(2)}+\phi_{WE,2}^{(11,2)}+\phi_{WE,2}^{(12,2)}.$$

C. Assumed Group-2 bubble shape and bubble number density distribution

Group-2 bubbles consist of cap and slug bubbles. Bubble shapes are subject to the wall effects when the diameter ratio $D_{b,cross}/D$ exceeds certain limits, where $D_{b,cross}$ is the bubble cross sectional diameter, and D is the tube diameter. In addition, there are two important parameters that are considered crucial for determining the bubble shape. They are the viscosity number given by $N_{\mu f}=\mu_f\Big/\left(\rho_f\sigma\sqrt{\sigma/g\Delta\rho}\right)^{1/2}$, and the length-scale ratio number given by $D^*=D\Big/\sqrt{\sigma/g\Delta\rho}$. According to Clift et al. (1978), when $D_{b,cross}/D\le 0.6$, the walls cause little deformation on the cap bubble shape as in an infinite medium. In this case, the shape of cap bubbles can be closely approximated as a segment of a sphere, and the wake angle is nearly 50°. When the diameter ratio $D_{b,cross}/D$ exceeds a value of about 0.6, the tube diameter becomes the controlling length governing the frontal shape of a bubble and then the bubble is called a slug bubble. The definitions of the geometrical parameters, including cross-sectional radius, a, the bubble height, h, and the wake angle, θ_w, are shown in Fig.11-4. It is shown (Clift et al., 1978) that the slug can be considered to be composed of two parts, a rounded nose region whose shape is independent of the slug length and a near-cylindrical section that is surrounded by an annular film of the liquid. It is also verified that for $N_{\mu f}\le 0.032$ and $D^*>10$, the viscosity and surface tension forces are negligible and the bubble shape on the potential flow theory can be well applied. The air-water flow in a moderate diameter tube ($N_{\mu f}=2.36\times10^{-3}$ and $D^*\cong19$ for a 50.8 mm-diameter tube) satisfies the above requirement. Therefore, the bubble shape can be predicted based on an application of the Bernoulli equation (Mishima and Ishii, 1984).

A simplified bubble number density distribution is given in Fig.11-5. It is assumed that all the bubble groups have flat number density distributions in the corresponding bubble volume range. The values of the distribution

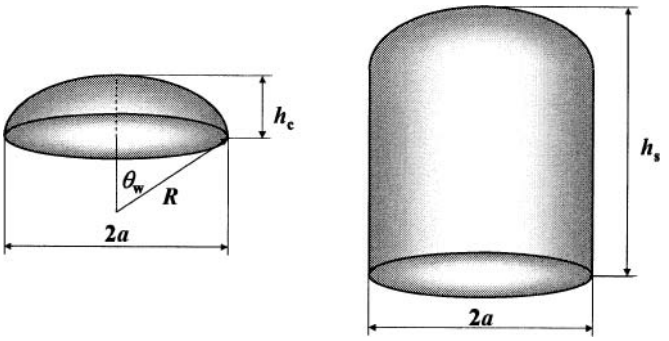

Figure 11-4. Definition of the geometrical parameters for cap and Taylor bubbles (Fu and Ishii, 2002a)

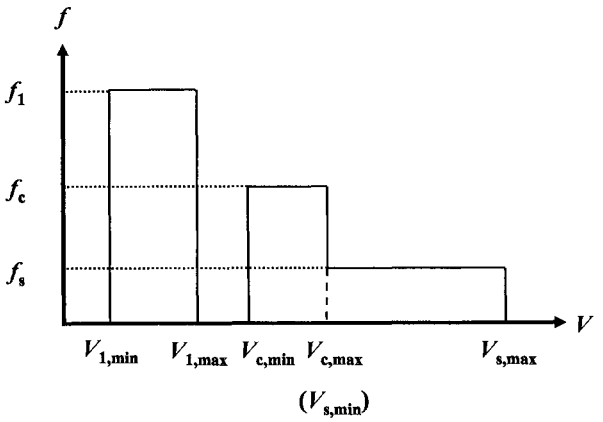

Figure 11-5. Illustration of the simplified bubble number density distribution (Fu and Ishii, 2002a)

function are denoted as f_1, f_c, and f_s for Group-1 bubbles, cap bubbles, and slug bubbles, respectively.

D. Summary of modeled source and sink terms

The modeled source and sink terms are summarized as follows. In the one-dimensional formulation, all the two-phase parameters such as α_g, a_i, and D_{Sm} are area-averaged values. For simplicity, the $\langle\ \rangle$ signs standing for the area-average are omitted in the following formulations.

Bubble coalescence due to random collision

$$\phi_{RC}^{(1)} = \left\langle \delta A_{i1}^{(11,1)} \right\rangle_R R_{RC}^{(1)} \tag{11-130}$$

$$\phi_{RC,1}^{(11,2)} = \left\langle \delta A_{i1}^{(11,2)} \right\rangle_R R_{RC}^{(1)} \tag{11-131}$$

$$\phi_{RC,2}^{(11,2)} = \left\langle \delta A_{i2}^{(11,2)} \right\rangle_R R_{RC}^{(1)} \tag{11-132}$$

$$\eta_{RC}^{(11,2)} = \left\langle \delta V^{(11,2)} \right\rangle_R R_{RC}^{(1)} \tag{11-133}$$

where

$$R_{RC}^{(1)} = C_{RC} \left[\frac{u_t {n_{b1}}^2 {D_{Sm1}}^2}{\alpha_{g1,\max}^{1/3} \left(\alpha_{g1,\max}^{1/3} - {\alpha_{g1}}^{1/3} \right)} \right] \times \left[1 - \exp\left(-C_T \frac{\alpha_{g1,max}^{1/3} \alpha_{g1}^{1/3}}{\alpha_{g1,\max}^{1/3} - \alpha_{g1}^{1/3}} \right) \right] \tag{11-134}$$

$$n_{b1} = \frac{1}{36\pi} \frac{a_{i1}^3}{\alpha_{g1}^2} \tag{11-135}$$

The turbulent fluctuation velocity (or root mean-squared velocity), u_t^2, is composed of the isotropic turbulence intensity, $u_{t,isot}^2$ and the wake turbulence intensity, $u_{t,wake}^2$, as

$$u_t^2 = u_{t,isot}^2 + u_{t,wake}^2 \tag{11-136}$$

$$u_{t,isot}^2 = \left(\varepsilon D_{Sm1} \right)^{2/3} \tag{11-137}$$

$$u_{t,wake}^2 = 0.056 C_g \left(\frac{D^3}{V_s^*}\right)^{1/2} \kappa_{fr} \tag{11-138}$$

where

$$C_g \equiv \sqrt{\frac{2g\Delta\rho}{\rho_f}} \tag{11-139}$$

$$V_s^* \equiv \frac{V_{s,min}}{V_{s,max}} \tag{11-140}$$

$$\kappa_{fr} = 1 - \exp\left(-\frac{C_{fr} V_s^{*1/2}}{D^{1/2}}\right). \tag{11-141}$$

Here, the constant C_{fr} is set at 1.8536. When $D_{Sm1} > 8.3338 \times 10^{-3}$ m,

$$\left\langle \delta A_{i1}^{(11,1)} \right\rangle_R = D_{Sm1}^2 \left[-3.142 D_{c1}^{*3} + 2.183 D_{c1}^{*5} - 0.395 D_{c1}^{*8} + 3.392 \left(0.579 D_{c1}^{*3} - 1\right)^{8/3} \right] \tag{11-142}$$

$$\left\langle \delta A_{i1}^{(11,2)} \right\rangle_R = D_{Sm1}^2 \left[8.82 + 2.035 \left(0.579 D_{c1}^{*3} - 1\right)^{8/3} - 5.428 D_{c1}^{*3} \right] \tag{11-143}$$

$$\left\langle \delta A_{i2}^{(11,2)} \right\rangle_R = D_{Sm1}^2 \left(6.462 - 2.182 D_{c1}^{*5} + 0.395 D_{c1}^{*8}\right) \tag{11-144}$$

$$\left\langle \delta V^{(11,2)} \right\rangle_R = D_{Sm1}^3 \xi \left(0.603 + 0.349 D_{c1}^{*3}\right) \tag{11-145}$$

$$\xi = 2\left(1 - 0.2894 D_{c1}^{*3}\right)^2 . \tag{11-146}$$

Otherwise,

$$\left\langle \delta A_{i1}^{(11,1)} \right\rangle_R = 1.001 D_{Sm1}^2 \tag{11-147}$$

and $\left\langle \delta A_{i1}^{(11,2)} \right\rangle_R$, $\left\langle \delta A_{i2}^{(11,2)} \right\rangle_R$, $\left\langle \delta V^{(11,2)} \right\rangle_R$ are all equal to zero.

Bubble coalescence due to wake entrainment

$$\phi_{WE}^{(1)} = \left\langle \delta A_{i1}^{(11,1)} \right\rangle_R R_{WE}^{(1)} \tag{11-148}$$

$$\phi_{WE,1}^{(11,2)} = \left\langle \delta A_{i1}^{(11,2)} \right\rangle_R R_{WE}^{(1)} \tag{11-149}$$

$$\phi_{WE,2}^{(11,2)} = \left\langle \delta A_{i2}^{(11,2)} \right\rangle_R R_{WE}^{(1)} \tag{11-150}$$

$$\phi_{WE,1}^{(12,2)} = -C_{WE}^{(12,2)} K_{WE,1}^{(12,2)} V_s^{*1/2} \frac{\alpha_{g1}\alpha_{g2}}{1-\alpha_{g2}} \kappa_{fr} D_{Sm1}^{-1} \tag{11-151}$$

$$\phi_{WE,2}^{(12,2)} = C_{WE}^{(12,2)} K_{WE,2}^{(12,2)} V_s^{*1/2} \frac{\alpha_{g1}\alpha_{g2}}{1-\alpha_{g2}} \kappa_{fr} \tag{11-152}$$

$$\phi_{WE}^{(2)} = -C_{WE}^{(2)} K_{WE}^{(2)} \alpha_{g2} \left[1 - \exp\left(\frac{-2331\alpha_{g2} V_s^{*2}}{D^5}\right)\right] \times \left[\exp\left(\frac{0.06 C_l \left(\alpha_{m2}/\alpha_{g2} - 1\right)}{V_s^*}\right) - 1\right]^{-1} \tag{11-153}$$

$$\eta_{WE}^{(11,2)} = \left\langle \delta V^{(11,2)} \right\rangle_R R_{WE}^{(1)} \tag{11-154}$$

$$\eta_{WE}^{(12,2)} = C_{WE}^{(12,2)} K_{WE}^{(12,2)} V_s^{*1/2} \frac{\alpha_{g1}\alpha_{g2}}{1-\alpha_{g2}} \kappa_{fr} \tag{11-155}$$

where

$$R_{WE}^{(1)} = C_{WE} C_D^{1/3} n_{b1}^2 D_{Sm1}^2 v_{r1} \tag{11-156}$$

$$v_{r1} \approx \sqrt{\frac{gD_{Sm1}}{3C_D}\frac{\Delta\rho}{\rho_f}} \tag{11-157}$$

$$C_D = \frac{2}{3} D_{Sm1} \sqrt{\frac{g\Delta\rho}{\sigma}} \left[\frac{1+17.67\left(1-\alpha_{g1}\right)^{2.6}}{18.67\left(1-\alpha_{g1}\right)^3} \right]^2 \tag{11-158}$$

$$K_{WE,1}^{(12,2)} = 3\pi C_g D^{1/2} \tag{11-159}$$

$$K_{WE,2}^{(12,2)} = 2\pi C_g D^{-1/2} \alpha_{m2}^{-1/2} \tag{11-160}$$

$$K_{WE}^{(2)} = 10.24 D^{3/2} \tag{11-161}$$

$$K_{WE}^{(12,2)} = 0.5\pi C_g D^{1/2} \tag{11-162}$$

$\left\langle \delta A_{i1}^{(11,2)} \right\rangle_R$, $\left\langle \delta A_{i1}^{(11,2)} \right\rangle_R$, $\left\langle \delta A_{i2}^{(11,2)} \right\rangle_R$, and $\left\langle \delta V^{(11,2)} \right\rangle_R$ are the same as those in Eqs.(11-142)-to-(11-145) and (11-147). The maximum cross-sectional void fraction of a slug bubble, α_{m2}, can be specified as 0.81 for most conditions and C_l is the adjustable parameter determined to be 0.1.

Bubble breakup due to turbulent impact

$$\phi_{TI}^{(1)} = \begin{cases} \dfrac{C_{TI}}{18}\left(\dfrac{u_t a_{i1}^{\ 2}}{\alpha_{g1}}\right)\left(1-\dfrac{We_{crit}}{We^*}\right)^{1/2}\exp\left(-\dfrac{We_{crit}}{We^*}\right), \\ We^* > We_{crit} \\ 0, \ \ We^* \le We_{crit} \end{cases} \tag{11-163}$$

where We is the Weber number defined by

$$We^* \equiv \frac{\rho_f u_t^2 D_{Sm1}}{\sigma} \tag{11-164}$$

$$\phi_{TI}^{(2)} = C_{TI2} K_{TI}^{(2)} \alpha_{g2} \varepsilon^{1/3} V_s^* \left(\frac{1-\alpha_{g1}-\alpha_{g2}}{1-\alpha_{g2}}\right) \tag{11-165}$$

where

$$\begin{aligned} K_{TI}^{(2)} &= D^{-1}\left[1-\left(\frac{D_c}{\alpha_{2,\max}^{1/2} D}\right)^{5/3}\right] \\ &\times\left[14.38+1.57\alpha_{m2}^{-2/3}\left(\frac{D_{crit}}{D}\right)^{4/3}-15.95\alpha_{m2}^{-1/6}\left(\frac{D_{crit}}{D}\right)^{1/3}\right] \end{aligned} \tag{11-166}$$

V_s^* can be determined by

$$D_{Sm2} = \frac{1.35D}{1+6.86V_s^*-2.54V_s^{*2}}. \tag{11-167}$$

It is observed from experiments that for moderate and small diameter pipes, the $\phi_{TI}^{(2)}$ term is very small compared with other three mechanisms. Therefore, it could be neglected to simplify the equation for application (Fu and Ishii, 2002b).

Bubble breakup due to shearing-off

$$\phi_{SO,1}^{(2,1)} = C_{SO} K_{SO,1}^{(2,1)} \alpha_{g2} V_s^{*-4/5} \left(1 - 0.6535\kappa_{bl}\right) \xi_{SO} \kappa_{fr}^{\ 2} \tag{11-168}$$

$$\phi_{SO,2}^{(2,1)} = -C_{SO} K_{SO,2}^{(2,1)} \alpha_{g2} V_s^{*-1/5} \left(1 - 0.6474\kappa_{bl}\right) \kappa_{fr}^{4/5} \tag{11-169}$$

$$\eta_{SO}^{(2,1)} = C_{SO} K_{SO}^{(2,1)} \alpha_{g2} V_s^{*-1/5} \left(1 - 0.6474\kappa_{bl}\right) \kappa_{fr}^{4/5} \tag{11-170}$$

where

$$\xi_{SO} = \left[1 - \exp\left(-\gamma_{SO}\left(\frac{\alpha_{m2}}{\alpha_{m2} - \alpha_{g2}}\right)^{\beta_{SO}} \frac{We_{crit}}{We_1}\right)\right]^{-1} \tag{11-171}$$

$$\kappa_{bl} = \left(D^{-0.3} \alpha_{m2}^{-0.5} \nu_g^{0.2} C_g^{-0.2} V_s^{*-0.7} \kappa_{fr}^{-0.2}\right)^{1/7} \tag{11-172}$$

$$K_{SO,1}^{(2,1)} = 0.5755 C_g^{\ 2} \nu_g^{1/5} \left(\frac{\rho_f}{\sigma D}\right)^{3/5} \tag{11-173}$$

$$K_{SO,2}^{(2,1)} = 4.4332 \alpha_{g2} \nu_g^{1/5} D^{-9/5} \alpha_{m2}^{1/2} C_g^{\ 4/5} \tag{11-174}$$

$$K_{SO}^{(2,1)} = 1.1083 \nu_g^{1/5} D^{-4/5} C_g^{\ 4/5} \tag{11-175}$$

where ν_g is the kinematic viscosity of the gas phase. The values of the coefficients in the source and sink terms are listed in Table 11-2.

1.3.3 Source and sink terms modeled by Sun et al. (2004a)

Sun et al. (2004a) developed the two-group interfacial area transport equation for bubbly flow, cap-turbulent flow, and churn-turbulent flows in a confined channel and evaluated it using a vertical air-water flow data taken

Table 11-3. List of intra- and inter-group interaction mechanisms in the model by Sun et al. (2004a; 2004b)

Symbols	Mechanisms	Interaction	Parameters
$\phi_{RC}^{(1)}$	Random collision	(1)+(1)→(1)	$C_{RC}^{(1)}$=0.005, $C_{RC}^{(12,2)}$=0.005
$\phi_{RC}^{(11,2)}$	Random collision	(1)+(1)→(2)	$C_{RC}^{(2)}$=0.005 C_{RC1}=3.0
$\phi_{RC}^{(12,2)}$	Random collision	(1)+(2)→(2)	C_{RC2}=3.0
$\phi_{RC}^{(2)}$	Random collision	(2)+(2)→(2)	$C_{WE}^{(1)}$=0.002, $C_{WE}^{(12,2)}$=0.002
$\phi_{WE}^{(1)}$	Wake entrainment	(1)+(1)→(1)	$C_{WE}^{(2)}$=0.005
$\phi_{WE}^{(11,2)}$	Wake entrainment	(1)+(1)→(2)	$C_{TI}^{(1)}$=0.03, $C_{TI}^{(2)}$=0.02
$\phi_{WE}^{(12,2)}$	Wake entrainment	(1)+(2)→(2)	$We_{crit,TI1}$=6.5, $We_{crit,TI2}$=7.0
$\phi_{WE}^{(2)}$	Wake entrainment	(2)+(2)→(2)	C_{SO}=3.8×10^{-5}, C_d=4.80
$\phi_{TI}^{(1)}$	Turbulent impact	(1)→(1)+(1)	$We_{crit,SO}$=4500
$\phi_{TI}^{(2,11)}$	Turbulent impact	(2)→(1)+(1)	
$\phi_{TI}^{(2,12)}$	Turbulent impact	(2)→(1)+(2)	
$\phi_{TI}^{(2)}$	Turbulent impact	(2)→(2)+(2)	
$\phi_{SO}^{(2,12)}$	Shearing-off	(2)→(2)+(1)	
$\phi_{SI}^{(2)}$	Surface instability	(2)→(2)+(2)	

in a rectangular channel with the width, W, of 200 mm and the gap, G, of 10 mm. No stable slug flow regime was observed in the test section due to the large width of the test section (Sun et al., 2004a). In what follows, the classification of interfacial area transport mechanisms and the modeled source and sink terms are explained briefly.

A. Classification of interfacial area transport mechanisms

Sun et al. (2004a) adopted five major bubble interactions: (1) the coalescence due to random collisions driven by turbulence; (2) the coalescence due to wake entrainment; (3) the breakup upon the impact of turbulent eddies; (4) the breakup due to shearing-off; and (5) the breakup of large cap bubbles due to flow instability on the bubble surface. Fourteen terms listed in Table 11-3 are considered as source and sink terms in the

two-group interfacial area transport equation to be applied at the bubbly, cap-turbulent and churn-turbulent flows in a confined channel.

B. Simplified two-group interfacial area transport equation

Here, an isothermal flow condition is assumed. Thus, two-group interfacial area transport equation is simplified as

$$\frac{\partial\left(\alpha_{g1}\rho_g\right)}{\partial t}+\nabla\cdot\left(\alpha_{g1}\rho_g\boldsymbol{v}_{g1}\right)=-\rho_g\left[\eta_{RC,2}^{(11,2)}+\eta_{RC,2}^{(12,2)}+\eta_{WE,2}^{(11,2)}\right.$$
$$\left.+\eta_{WE,2}^{(12,2)}+\eta_{SO,2}^{(2,12)}+\eta_{TI,2}^{(2,1)}+\chi\left(D_{c1}^{*}\right)^3\left\{\frac{\partial\alpha_{g1}}{\partial t}+\nabla\cdot\left(\alpha_{g1}\boldsymbol{v}_{g1}\right)\right\}\right] \tag{11-176}$$

$$\frac{\partial a_{i1}}{\partial t}+\nabla\cdot\left(a_{i1}\boldsymbol{v}_{i1}\right)$$
$$=\left\{\frac{2}{3}-\chi\left(D_{c1}^{*}\right)^2\right\}\frac{a_{i1}}{\alpha_{g1}}\left[\frac{\partial\alpha_{g1}}{\partial t}+\nabla\cdot\left(\alpha_{g1}\boldsymbol{v}_{g1}\right)\right] \tag{11-177}$$
$$+\phi_{RC}^{(1)}+\phi_{RC,1}^{(12,2)}+\phi_{WE}^{(1)}+\phi_{WE,1}^{(12,2)}+\phi_{TI}^{(1)}+\phi_{TI,1}^{(2,1)}+\phi_{SO,1}^{(2,12)}$$

$$\frac{\partial a_{i2}}{\partial t}+\nabla\cdot\left(a_{i2}\boldsymbol{v}_{i2}\right)=\frac{2}{3}\frac{a_{i2}}{\alpha_{g2}}\left[\frac{\partial\alpha_{g2}}{\partial t}+\nabla\cdot\left(\alpha_{g2}\boldsymbol{v}_{g2}\right)\right]$$
$$+\chi\left(D_{c1}^{*}\right)^2\frac{a_{i1}}{\alpha_{g1}}\left[\frac{\partial\alpha_{g1}}{\partial t}+\nabla\cdot\left(\alpha_{g1}\boldsymbol{v}_{g1}\right)\right]+\phi_{RC,2}^{(11,2)}+\phi_{RC,2}^{(12,2)} \tag{11-178}$$
$$+\phi_{RC}^{(2)}+\phi_{WE,2}^{(11,2)}+\phi_{WE,2}^{(12,2)}+\phi_{WE}^{(2)}+\phi_{TI,2}^{(2)}+\phi_{SO,2}^{(2,12)}+\phi_{SI}^{(2)}.$$

C. Assumed Group-2 bubble shape and bubble-number density distribution

In order to model source and sink terms analytically, the bubble shape should be simplified. For Group-1 bubbles, spherical shape can be assumed. For Group-2 bubbles, however, the unique geometry of the test section of interest should be accounted for. Since the boundary between Group-1 and Group-2 bubbles defined by Eq.(11-115) is approximately 10 mm in an adiabatic air-water system at atmospheric pressure, the cap bubbles are assumed to be sandwiched between the two parallel flat walls such that the cap bubbles have a thickness of G, as shown in Fig.11-6. Here, R and $2a$

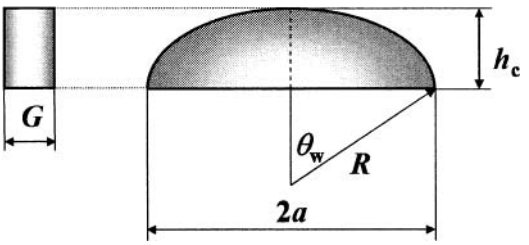

Figure 11-6. Definition of the geometrical parameters for a cap bubble (Sun et al., 2004a)

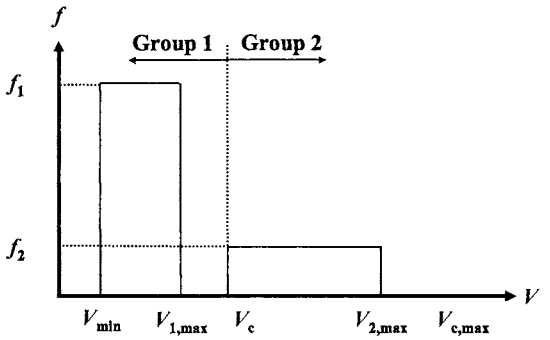

Figure 11-7. Illustration of the simplified bubble number density distribution (Sun et al., 2004)

are the radius of curvature and the base width of a cap bubble, and θ_w is the wake angle. A 50° wake angle is assumed as a reasonable approximation for all Group-2 bubbles in the flow conditions of interest in view of the wake angle correlation given by Clift et al. (1978). Furthermore, in view of the characteristic feature of the confined flows as well as the underlying physics, $2a$ is chosen as the characteristic length that determines the group boundary and the maximum stable bubble size.

A simplified bubble number density distribution is given in Fig.11-7. It is assumed that all the bubble groups have flat number density distributions in the corresponding bubble volume range. The values of the distribution function are denoted as f_1 and f_2 for Group-1 bubbles and Group-2 bubbles, respectively. In the figure, V_{min} is the volume for the minimum bubbles in the system, and $V_{c,max}$ is the volume of the maximum stable bubble, which corresponds to

$$D_{c,\max} = 40\sqrt{\frac{\sigma}{g\Delta\rho}}. \tag{11-179}$$

It should be noted, however, that bubbles of this size might not exist in the system and $D_{c,max}$ solely provides an upper limit for the maximum bubble size possible, beyond which the bubbles are assumed to disintegrate instantaneously. $V_{1,max}$ and $V_{2,max}$ are the maximum bubble volumes for Group 1 and Group 2, respectively, for a given flow condition by assuming the uniform bubble number density distribution. Furthermore, V_c is the critical bubble volume at the boundary for Group-1 and Group-2 bubbles, which corresponds to D_{crit} beyond which bubbles become cap-shaped and are categorized as Group-2 bubbles. The boundary between Group-1 and Group-2 bubbles can be determined for the narrow channel by

$$D_{crit} = 1.7G^{1/3}\left(\frac{\sigma}{g\Delta\rho}\right)^{1/3} \tag{11-180}$$

where D_{crit} is the volumetric equivalent diameter of a bubble at the boundary between Group-1 and Group-2 bubbles.

D. Summary of modeled source and sink terms

Bubble coalescence due to random collision

$$\phi_{RC}^{(1)} = -0.17C_{RC}^{(1)}\frac{\varepsilon^{1/3}\alpha_{g1}^{1/3}a_{i1}^{5/3}}{\alpha_{g1,max}^{1/3}\left(\alpha_{g1,max}^{1/3}-\alpha_{g1}^{1/3}\right)} \times\left[1-\exp\left(-C_{RC1}\frac{\alpha_{g1,max}^{1/3}\alpha_{g1}^{1/3}}{\alpha_{g1,max}^{1/3}-\alpha_{g1}^{1/3}}\right)\right] \tag{11-181}$$

$$\phi_{RC,1}^{(12,2)} = -4.85C_{RC}^{(12,2)}\varepsilon^{1/3}\frac{a_{i1}\alpha_{g1}^{2/3}\alpha_{g2}^{2}}{R_{2,max}^{2/3}} \times\left[1-\exp\left(-C_{RC1}\frac{\alpha_{g1,max}^{1/3}\alpha_{g1}^{1/3}}{\left(\alpha_{g1,max}^{1/3}-\alpha_{g1}^{1/3}\right)}\right)\right] \tag{11-182}$$

where $R_{2,max}$ is the radius of curvature of the maximum bubble in the system by assuming a uniform bubble number density distribution as

$$R_{2,max} \simeq 1.915 D_{Sm,2} \tag{11-183}$$

for the application of Sun et al. (2004a).

$$\begin{aligned}\phi_{RC,2}^{(11,2)} &= 0.68 C_{RC}^{(1)} \varepsilon^{1/3} \frac{\alpha_{g1}^2 a_{i1}^{2/3}}{\alpha_{g1,max}^{2/3} G} \\ &\times \left[1 - \exp\left(-C_{RC1} \frac{\alpha_{g1,max}^{1/3} \alpha_{g1}^{1/3}}{\alpha_{g1,max}^{1/3} - \alpha_{g1}^{1/3}}\right)\right] \\ &\times \left[1 + 0.7 G^{7/6} \left(\frac{a_{i1}}{\alpha_{g1}}\right)^{1/2} \left(\frac{\sigma}{g \Delta \rho}\right)^{-1/3}\right] \left(1 - \frac{2}{3} D_{c1}^*\right) \\ &\text{for } D_{c1}^* < 1.5\end{aligned} \tag{11-184}$$

$$\begin{aligned}\phi_{RC,2}^{(12,2)} &= 13.6 C_{RC}^{(12,2)} \varepsilon^{1/3} \frac{\alpha_{g1}^{5/3} \alpha_{g2}^2}{R_{2,max}^{2/3} G} \left(1 + \frac{10.3 G}{R_{2,max}}\right) \\ &\times \left[1 - \exp\left(-C_{RC1} \frac{\alpha_{g1,max}^{1/3} \alpha_{g1}^{1/3}}{\left(\alpha_{g1,max}^{1/3} - \alpha_{g1}^{1/3}\right)}\right)\right]\end{aligned} \tag{11-185}$$

$$\begin{aligned}\phi_{RC}^{(2)} &= -13.6 C_{RC}^{(2)} \frac{\alpha_{g2}^2 \varepsilon^{1/3}}{W^2 G} R_{2,max}^{4/3} \left(1 - 2.0 R_c^{*2} + \frac{9.0 G}{R_{2,max}}\right) \\ &\times \left[1 - \exp\left(-C_{RC2} \alpha_{g2}^{1/2}\right)\right]\end{aligned} \tag{11-186}$$

where

$$R_c^* \equiv \frac{D_{crit}/2}{R_{2,max}} \tag{11-187}$$

$$\eta_{RC,2}^{(11,2)} = 3.4C_{RC}^{(1)} \frac{\varepsilon^{1/3}\alpha_{g1}^{2}a_{i1}^{2/3}}{\alpha_{g1,max}^{2/3}} \times\left[1-\exp\left(-C_{RC1}\frac{\alpha_{g1,max}^{1/3}\alpha_{g1}^{1/3}}{\alpha_{g1,max}^{1/3}-\alpha_{g1}^{1/3}}\right)\right]\left(1-\frac{2}{3}D_{c1}^{*}\right) \quad (11\text{-}188)$$

for $D_{c1}^{*} < 1.5$

$$\eta_{RC,2}^{(12,2)} = 4.85C_{RC}^{(12,2)}\varepsilon^{1/3}\frac{\alpha_{g1}^{5/3}\alpha_{g2}^{2}}{R_{2,max}^{2/3}} \times\left[1-\exp\left(-C_{RC1}\frac{\alpha_{g1,max}^{1/3}\alpha_{g1}^{1/3}}{\left(\alpha_{g1,max}^{1/3}-\alpha_{g1}^{1/3}\right)}\right)\right] \quad (11\text{-}189)$$

Bubble coalescence due to wake entrainment

$$\phi_{WE}^{(1)} = -0.27C_{WE}^{(1)}u_{r1}C_{D1}{}^{1/3}a_{i1}^{2} \quad (11\text{-}190)$$

$$\phi_{WE,1}^{(12,2)} = -4.35C_{WE}^{(12,2)}\sqrt{gC_{D2}G}\frac{a_{i1}\alpha_{g2}}{R_{2,max}} \quad (11\text{-}191)$$

$$\phi_{WE,2}^{(11,2)} = 1.08C_{WE}^{(11,2)}u_{r1}C_{D1}{}^{1/3}\frac{\alpha_{g1}a_{i1}}{G}\left(1-\frac{2}{3}D_{c1}^{*}\right) \times\left[1+0.7G^{7/6}\left(\frac{a_{i1}}{\alpha_{g1}}\right)^{1/2}\left(\frac{\sigma}{g\Delta\rho}\right)^{-1/3}\right] \quad (11\text{-}192)$$

for $D_{c1}^{*} < 1.5$

$$\phi_{WE,2}^{(12,2)} = 26.1C_{WE}^{(12,2)}\alpha_{g1}\alpha_{g2}\sqrt{\frac{gC_{D2}}{G}}\frac{1}{R_{2,max}}\left(1+4.31\frac{G}{R_{2,max}}\right) \quad (11\text{-}193)$$

$$\phi_{WE}^{(2)} = -15.9 C_{WE}^{(2)} \frac{\alpha_{g2}^2}{R_{2,max}^2} \sqrt{C_D g G} \left(1 + 0.51 R_c^*\right) \tag{11-194}$$

$$\eta_{WE,2}^{(11,2)} = 5.40 C_{WE}^{(11,2)} u_{r1} C_{D1}^{1/3} \alpha_{g1} a_{i1} \left(1 - \frac{2}{3} D_{c1}^*\right) \text{ for } D_{c1}^* < 1.5 \tag{11-195}$$

$$\eta_{WE,2}^{(12,2)} = 4.35 C_{WE}^{(12,2)} \sqrt{C_{D2} g G} \frac{\alpha_{g1} \alpha_{g2}}{R_{2,max}} \tag{11-196}$$

Bubble breakup due to turbulent impact

$$\phi_{TI}^{(1)} = \begin{cases} 0.12 C_{TI}^{(1)} \varepsilon^{1/3} \left(1 - \alpha_g\right) \dfrac{a_{i1}^{5/3}}{\alpha_{g1}^{2/3}} \exp\left(-\dfrac{We_{crit,TI1}}{We_1}\right) \\ \qquad \times \sqrt{1 - \dfrac{We_{crit,TI1}}{We_1}}, \quad We_1 > We_{crit,TI1} \\ 0, \quad We_1 \le We_{crit,TI1} \end{cases} \tag{11-197}$$

$$\phi_{TI,1}^{(2,1)} = 2.71 C_{TI}^{(2)} \alpha_{g2} \left(1 - \alpha_g\right) \frac{\varepsilon^{1/3} G^{2/3} R_c^{*5/3} \left(1 - R_c^{*5/3}\right)}{R_{2,max}^{7/3}} \times \exp\left(-\frac{We_{crit,TI2}}{We_2}\right) \sqrt{1 - \frac{We_{crit,TI2}}{We_2}} \tag{11-198}$$

$$\phi_{TI,2}^{(2)} = 1.4 C_{TI}^{(2)} \alpha_{g2} \frac{\varepsilon^{1/3} G}{R_{2,max}^{8/3}} \left(1 - \alpha_g\right)\left(1 - 2R_c^*\right) \times \exp\left(-\frac{We_{crit,TI2}}{We_2}\right) \sqrt{1 - \frac{We_{crit,TI2}}{We_2}} \tag{11-199}$$

$$\eta_{TI,2}^{(2,1)} = -0.34 C_{TI}^{(2)} \alpha_{g2} \left(1-\alpha_g\right) \frac{G\varepsilon^{1/3} R_c^{*7/3} \left(1-R_c^{*5/3}\right)}{R_{2,max}^{5/3}} \times \exp\left(-\frac{We_{crit,TI2}}{We_2}\right) \sqrt{1-\frac{We_{crit,TI2}}{We_2}} \tag{11-200}$$

Bubble breakup due to shearing off

$$\phi_{SO,1}^{(2,12)} = 64.51 C_{SO} C_d^{\,2} \frac{\alpha_{g2} v_{rb}}{G R_{2,max}} \left[1-\left(\frac{We_{crit,SO}}{We_{2,max}}\right)^3\right] \tag{11-201}$$

where v_{rb} and $We_{crit,SO}$ are the relative velocity of the large bubble with respect to the liquid film near the cap bubble base and the critical Weber number, respectively, and $We_{2,max}$ is defined by

$$We_{2,max} \equiv \frac{2\rho_f v_{rb}^2 R_{2,max}}{\sigma} \tag{11-202}$$

In upward flow in round tubes, when a large cap or slug bubble rises, the liquid phase is pushed away and flows downward as a liquid film between the bubble side interface and the wall. However, in the flow channel considered by Sun et al. (2004a), when a large cap bubble rises, the liquid film between the bubble side interface and the wall may remain almost stagnant since more free space is available for the liquid phase in the width direction of the flow channel. This may be even truer when the cap bubble velocity is high and the shearing-off occurs. In view of this, the relative velocity of the cap bubble with respect to the liquid film around the bubble base, v_{rb}, may be estimated by the velocity of Group-2 bubbles in the main flow direction.

$$\phi_{SO,2}^{(2,12)} = -21.50 C_{SO} C_d^{\,3} \left(\frac{\sigma}{\rho_f}\right)^{3/5} \frac{\alpha_{g2}}{v_{rb}^{1/5} G^{8/5} R_{2,max}} \times \left[1-\left(\frac{We_{crit,SO}}{We_{2,max}}\right)^3 + \frac{3.24G}{R_{2,max}} \left\{1-\left(\frac{We_{crit,SO}}{We_{2,max}}\right)^2\right\}\right] \tag{11-203}$$

$$\eta_{SO,2}^{(2,12)} = -10.75 C_{SO} C_d^{\,3} \left(\frac{\sigma}{\rho_f G}\right)^{3/5} \frac{\alpha_{g2}}{v_{rb}^{1/5} R_{m2}} \times \left\{1 - \left(\frac{We_{crit,SO}}{We_{m2}}\right)^3\right\} \tag{11-204}$$

Bubble breakup due to surface instability

$$\phi_{SI}^{(2)} = 1.25 \alpha_{g2}^2 \left(\frac{\sigma}{g\Delta\rho}\right)^{-1} \left[C_{RC}^{(2)} \frac{\varepsilon^{1/3}}{W^2} \left(\frac{\sigma}{g\Delta\rho}\right)^{7/6} \times \left\{1 - \exp\left(-C_{RC2} \alpha_{g2}^{1/2}\right)\right\} + 2.3 \times 10^{-4} C_{WE}^{(2)} \sqrt{C_D g G}\right] \tag{11-205}$$

The values of the coefficients in the source and sink terms are listed in Table 11-3.

Inter-group transfer coefficient at group boundary

The inter-group transfer coefficient at group boundary is determined experimentally as

$$\chi = 4.44 \times 10^{-3} \left(\frac{D_{Sm1}}{D_{crit}}\right)^{0.36} \alpha_{g1}^{\,-1.35}. \tag{11-206}$$

This correlation is obtained based on the limited experimental database (Sun et al., 2004a). Nevertheless, in general cap-turbulent and churn-turbulent flow, the value of α_{g1} is usually between 0.05 and 0.40. Therefore, the correlation may be applicable to most of these flow conditions since the database by which the correlation is developed covers the similar range of α_{g1}.